Time-Periodic Solutions of the Benjamin-Ono Equation

David M. Ambrose * Jon Wilkening †

April 23, 2008

Abstract

We present a spectrally accurate numerical method for finding non-trivial time-periodic solutions of non-linear partial differential equations. The method is based on minimizing a functional (of the initial condition and the period) that is positive unless the solution is periodic, in which case it is zero. We solve an adjoint PDE to compute the gradient of this functional with respect to the initial condition. We include additional terms in the functional to specify the free parameters, which, in the case of the Benjamin-Ono equation, are the mean, a spatial phase, a temporal phase and the real part of one of the Fourier modes at $t = 0$.

We use our method to study global paths of non-trivial time-periodic solutions connecting stationary and traveling waves of the Benjamin-Ono equation. As a starting guess for each path, we compute periodic solutions of the linearized problem by solving an infinite dimensional eigenvalue problem in closed form. We then use our numerical method to continue these solutions beyond the realm of linear theory until another traveling wave is reached (or until the solution blows up). By experimentation with data fitting, we identify the analytical form of the solutions on the path connecting the one-hump stationary solution to the two-hump traveling wave. We then derive exact formulas for these solutions by explicitly solving the system of ODE's governing the evolution of solitons using the ansatz suggested by the numerical simulations.

Key words. Periodic solutions, Benjamin-Ono equation, non-linear waves, solitons, bifurcation, continuation, optimal control, adjoint equation, spectral method

AMS subject classifications. 65K10, 37M20, 35Q53, 37G15

*Department of Mathematical Sciences, Clemson University, Clemson, SC 29634 (dambros@clemson.edu). This work was supported in part by the National Science Foundation through grant DMS-0707807.

†Department of Mathematics and Lawrence Berkeley National Laboratory, University of California, Berkeley, CA 94720 (wilken@math.berkeley.edu). This work was supported in part by the Director, Office of Science, Computational and Technology Research, U.S. Department of Energy under Contract No. DE-AC02-05CH11231.

1 Introduction

A fundamental problem in the theory of ordinary and partial differential equations is to determine whether the equation possesses time-periodic solutions. Famous examples of ordinary differential equations with periodic solutions include the Brusselator [FB85, Gov00, Str00] and the three-body problem [Are63, HNW00]. In partial differential equations, time-periodic solutions can be "trivial" stationary or traveling waves, or can be genuinely time-periodic. Such a problem can be studied in either the forced or unforced context. Forced problems include an external force in the PDE that is usually time-periodic; solutions with the same period are then sought. In the unforced problem, the period is one of the unknowns. In this work, we present a numerical method for finding genuinely time-periodic solutions of the unforced Benjamin-Ono equation with periodic boundary conditions. These new solutions have many remarkable properties, which we will describe.

Our work is motivated by the calculations of Hou, Lowengrub, and Shelley for the vortex sheet with surface tension [HLS94, HLS97], and by the analysis of Plotnikov, Toland and Iooss [PT01, IPT05] for the water wave. Hou, Lowengrub, and Shelley developed an efficient numerical method to solve the initial value problem for the vortex sheet with surface tension. They performed calculations for a variety of initial conditions and values of the surface tension parameter, and found many situations in which the solutions appear to be close to time-periodic. They did not, however, try to measure the deviation from time-periodicity or attempt to vary the initial conditions to reduce this deviation. Plotnikov, Toland, and Iooss have proved the existence of time-periodic water waves, without surface tension, in the case of either finite or infinite depth. This is proved using a version of the Nash-Moser implicit function theorem. Their work includes no computation of the water waves. We aim to get a firmer handle on these solutions with an explicit calculation. To this end, in the present work, we develop a general numerical method for finding time-periodic solutions of nonlinear systems of partial differential equations and eventually plan to use this method for the vortex sheet and water wave problems.

We chose the Benjamin-Ono equation as a first application for our numerical method because it is much less expensive to evolve than the vortex sheet with surface tension or the water wave, yet has many features in common with them, such as non-locality (due to the Hilbert transform in the former case and the Birkhoff-Rott integral in the latter two cases.) The Benjamin-Ono equation, developed in [Ben67, DA67, Ono75], is a model equation for the evolution of waves on deep water. It is a widely-studied dispersive equation, and much is known about solutions. It would be impossible to mention all results on Benjamin-Ono, but we mention, for example, that weak solutions exist for $u_0 \in L^2$ [Sau79, GV91], and

that the solution exists for all time if $u_0 \in H^1$ [Tao04]. Yet there is little in the literature about time-periodic solutions of Benjamin-Ono. We have discovered that the Benjamin-Ono equation has a rich family of non-trivial time-periodic solutions that act as rungs in a ladder connecting traveling waves with different speeds and wavelengths by creating or annihilating oscillatory humps that grow or shrink in amplitude until they become part of the stationary or traveling wave on the other side of the rung. The dynamics of these non-trivial solutions are often very interesting, sometimes resembling a low amplitude traveling wave superimposed on a larger carrier signal, and other times looking like a collection of interacting solitons that pass through each other or bounce off each other, depending on their relative amplitudes. By fitting our numerical data, we find that these solutions are all N-soliton solutions [Cas78, Cas80] with special initial conditions (that yield periodic orbits) and a modified mean to change their speeds; however, we did not take advantage of (or know about) this structure when we developed our numerical method.

We are aware of very few works on the existence of time-periodic solutions for water wave model equations. A. Crannell has demonstrated [Cra96] the existence of periodic, non-traveling, weak solutions of the Boussinesq equation using a generalization of the mountain pass lemma of Rabinowitz. Chen and Iooss have proved existence of time-periodic solutions in a two-way Boussinesq-type water wave model [CI05]. As in [PT01] and [IPT05], there is no computation of the solution in either of these studies. Cabral and Rosa have recently discovered a period-doubling cascade of periodic solutions for a damped and forced version of the Korteweg–de Vries equation [CR04]. They use a Fourier pseudospectral method for the spatial discretization and a first order semi-implicit scheme in time. To find periodic solutions, they use a secant method on a numerical Poincaré map. Whereas our approach is based on minimizing a functional that measures deviation from periodicity, they rely on the stability of the orbit to converge to a periodic solution. Also, they stop when they find a solution that returns to within one percent of its initial state, whereas we resolve our periodic solutions to 13-15 digits of accuracy, which allows us to study the analytic form of the solutions.

Water waves aside, many authors have investigated time-periodic solutions of other partial differential equations both numerically and analytically. For instance, Smiley proves existence of time-periodic solutions of a nonlinear wave equation on an unbounded domain [Smi89]; he also develops a numerical method for the same problem [Smi90]. On a finite domain, Brezis uses duality principles to prove the existence of periodic solutions of nonlinear vibrating strings in both the forced and unforced setting; see [Bre83]. Mawhin has written a survey article on periodic solutions of semilinear wave equations [Maw95], which includes many references. Pao has developed a numerical method for the solution of time-periodic

parabolic boundary-value problems [Pao01]. Pao gives various iterative schemes, but unlike the present work, these are not based on variational principles or the dual system. And of course, time-periodic solutions of systems of ordinary differential equations have also been widely studied, which is relevant here due to the ODE governing the evolution of N-soliton solutions; see e.g. [Rab78, Rab82, Zeh83, Dui84].

The closest numerical method to our own that we have found is due to Bristeau, Glowinski and Périaux [BGP98], who developed a least squares shooting method for numerical computation of time-periodic solutions of linear dynamical systems with applications in scattering phenomena in two and three dimensions; see also [GR06]. These authors employ methods of control theory to compute variational derivatives, and although they only apply their methods to linear problems, they mention that their techniques will also work on nonlinear problems. Our method can be considered an extension of their approach that focuses on the difficulties that arise due to non-linearity. In particular, we replace their conjugate gradient solver with a black-box minimization algorithm, (the BFGS method [NW99]), and include an additional penalty function to prescribe the values of the free parameters that describe the manifold of non-trivial time-periodic solutions. Without this penalty function, the basic method is only found to produce constant solutions and traveling waves.

This paper is organized as follows: In Section 2, we discuss spatially periodic stationary and traveling solutions of the Benjamin-Ono equation, the bifurcations from constant solutions to traveling waves, and the equation governing the evolution of solitons. In Section 3, we investigate time-periodic solutions of the linearized Benjamin-Ono equation; this is the linearization about the stationary solutions discussed previously. To analyze the linearized problem, we compute (numerically) the spectrum and eigenfunctions of the relevant linear operator and deduce their analytic form by trial and error; the resulting formulas can be verified rigorously (but we omit details). In Section 3.2, we discuss Liapunov-Schmidt theory and its limitations due to a small divisor problem. Using this theory as a guide, we expect stationary and traveling waves to bifurcate into four-parameter sheets of non-trivial time-periodic solutions parametrized by the mean, a spatial phase, a temporal phase and an essential bifurcation parameter. We give a symmetry argument to explain why we expect these periodic solutions to possess even spatial symmetry at $t = 0$, possibly after a phase shift in space and time. There may be symmetry-breaking bifurcations from these non-trivial solutions to even more complicated solutions, but we believe all bifurcations from stationary and traveling waves will be symmetric (up to a phase shift).

In Section 4, we describe our numerical method, which involves minimizing a non-negative functional that is zero if and only if the solution is periodic. We solve an adjoint PDE to compute the variational derivative of this functional with respect to perturbation of

the initial condition and use the BFGS minimization algorithm to minimize the functional. The Benjamin-Ono and adjoint equations are solved with a pseudo-spectral collocation method using a fourth order, semi-implicit Runge-Kutta scheme. We use a penalty function to rule out constant solutions and traveling waves, and to prescribe the free parameters of the manifold of non-trivial solutions; we then vary the essential bifurcation parameter to study the global properties of these non-trivial solutions. In the present work, we apply this method only to the Benjamin-Ono equation, but we are confident that this method is applicable to virtually any system of partial differential equations that possesses time-periodic solutions.

In Section 5, we use our method to study the global behavior of non-trivial time-periodic solutions far beyond the realm of validity of the linearization about stationary and traveling waves. We will follow one such path to discover that the one-hump stationary solution is connected to the two-hump traveling wave by a path of non-trivial time periodic solutions. In Section 6, we re-formulate the ODE governing the evolution of solitons to reveal an exact formula for the solutions on the path studied numerically in Section 5. Thus, unexpectedly, we have proved that non-trivial time-periodic solutions exist by exhibiting a family of them explicitly. In a follow-up paper [AW], we will classify all bifurcations from traveling waves, study the paths of non-trivial solutions connecting several of them, propose a conjecture explaining how they all fit together, and describe their analytic form to the extent that we are able. We end with a few concluding remarks in Section 7.

2 Stationary, Traveling and Soliton Solutions

We consider the Benjamin-Ono equation, with the following sign convention:

$$u_t = Hu_{xx} - uu_x. \tag{1}$$

Of course, the operator H is the Hilbert transform. Recall that the symbol of H is $\hat{H}(k) = -i\,\mathrm{sgn}(k)$. We consider the spatial domain $[0, 2\pi]$ with periodic boundary conditions. This equation possesses a two-parameter family of stationary solutions, namely

$$u(x) = \frac{1-3\beta^2}{1-\beta^2} + \frac{4\beta[\cos(x-\theta)-\beta]}{1+\beta^2-2\beta\cos(x-\theta)}, \qquad (-1<\beta<1,\ \theta\in\mathbb{R}). \tag{2}$$

These solutions have mean α, related to β via

$$\alpha(\beta) = \frac{1-3|\beta|^2}{1-|\beta|^2}, \qquad |\beta|^2 = \frac{1-\alpha}{3-\alpha}. \tag{3}$$

Changing the sign of β is equivalent to the phase shift $\theta \to \theta - \pi$. It is convenient to complexify β and define u_β to be the mean-zero part of (2) with $\beta \leftarrow |\beta|$, $\theta \leftarrow \arg\bar{\beta}$:

$$\text{stationary solution} = \alpha(\beta) + u_\beta(x), \qquad \beta = |\beta|e^{-i\theta} \in \Delta = \{z\in\mathbb{C} : |z|<1\}. \tag{4}$$

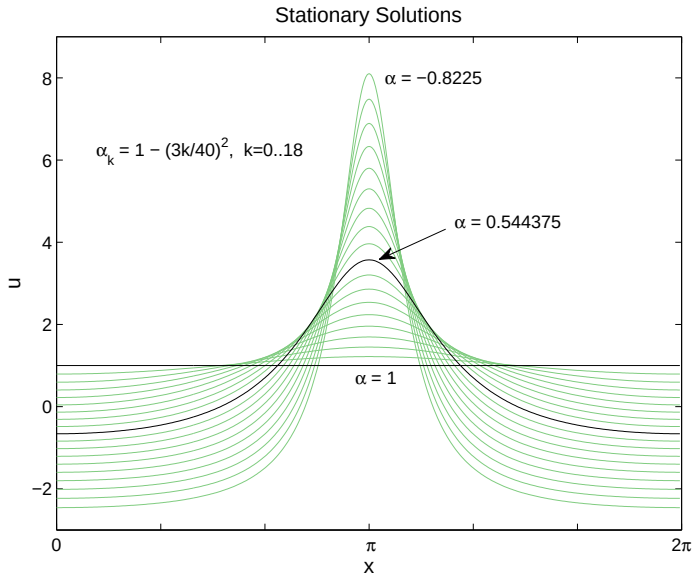

Figure 1: Stationary solutions of the Benjamin-Ono equation.

Note that the subscript β does not indicate a derivative here. Several stationary solutions with β real and negative are shown in Figure 1. The Fourier representation of u_β is simply

$$\hat{u}_{\beta,k} = \left\{ \begin{array}{ll} 2\bar{\beta}^{|k|}, & k < 0 \\ 0, & k = 0 \\ 2\beta^k, & k > 0 \end{array} \right\}, \tag{5}$$

where $\bar{\beta}$ is the complex conjugate of β. These functions $u_\beta(x)$ are the building blocks for the soliton solutions discussed below.

Note that the constant solution $u \equiv \alpha_0$ is also a stationary solution, as are the re-scaled solutions

$$u_{N,\beta}(x) = N\alpha(\beta) + Nu_\beta(Nx), \qquad (\beta \in \Delta,\ N = 1, 2, 3, \dots),$$

which have mean $\alpha_0 = N\alpha(\beta)$. If we restrict our attention to even solutions (with β real), we find that there is a pitchfork bifurcation at each positive integer. As α_0 changes from N^+ to N^-, the constant solution splits, yielding two additional (N-hump stationary) solutions, namely $u_{N,\beta}(x)$ with $\beta = 0^\pm$. The pitchfork would be obtained by plotting the real part of the Nth Fourier mode versus the mean, where we observe that the Fourier representation

of $u = u_{N,\beta}$ (for any $\beta \in \Delta$) is given by

$$\hat{u}_k = \begin{cases} N\alpha(\beta), & k = 0, \\ 2N\beta^{k/N}, & k \in N\mathbb{Z},\ k > 0, \\ 2N\bar{\beta}^{|k|/N}, & k \in N\mathbb{Z},\ k < 0, \\ 0 & \text{otherwise.} \end{cases} \tag{6}$$

If we do not restrict attention to even solutions, the phase shift θ acts as a second parameter connecting the two outer branches of the pitchfork into a two-dimensional, bowl-shaped sheet (plotting the real and imaginary parts of the Nth Fourier mode versus the mean).

In the bifurcation problem just described, we varied the mean α_0 and found bifurcations from constant solutions to stationary solutions at the positive integers. The remainder of this paper deals with bifurcation from these stationary solutions to non-trivial time-periodic solutions and their global continuation beyond the realm of linear theory. Rather than varying the mean, we will hold $\alpha_0 \in \mathbb{R}$ constant and use another quantity (such as the period T or the real part of one of the Fourier modes of u at $t = 0$) as the bifurcation parameter. As a first step, let us consider bifurcation from constant solutions to traveling waves holding $\alpha_0 \in \mathbb{R}$ constant and varying T.

All traveling wave solutions of the Benjamin-Ono equation can be found by applying a simple transformation to a stationary solution, and vice versa. Indeed, if $u(x,t)$ is any solution of (1), then

$$U(x,t) = u(x - ct, t) + c \tag{7}$$

is also a solution; thus, adding a constant c to a stationary solution causes it to travel to the right with speed c. We can parametrize these N-hump traveling waves by their mean $\alpha_0 \in \mathbb{R}$ and decay/phase parameter $\beta \in \Delta$:

$$u_{\alpha_0,N,\beta}(x,t) = u_{N,\beta}(x - ct) + c, \qquad \big(c = \alpha_0 - N\alpha(\beta)\big). \tag{8}$$

If we express the period $T = 2\pi/(N|c|)$ in terms of β and solve for β, we find that we can bifurcate from any constant solution $u \equiv \alpha_0$ to an N-hump traveling solution with the same mean. If $\alpha_0 < N$, a pitchfork from the constant solution occurs at $T_0 = 2\pi/[N(N - \alpha_0)]$; as we increase T from T_0 to ∞, $\alpha = [2\pi/(NT) + \alpha_0]/N$ decreases from 1 to α_0/N and $|\beta|$ varies from 0 to $\sqrt{(1 - \alpha_0/N)/(3 - \alpha_0/N)}$. Similarly, if $\alpha_0 > N$, a pitchfork occurs at $T_0 = 2\pi/[N(\alpha_0 - N)]$; as we *decrease* T from T_0 to 0, $\alpha = [\alpha_0 - 2\pi/(NT)]/N$ decreases from 1 to $-\infty$, and $|\beta|$ varies from 0 to 1. And if $\alpha_0 = N$, the situation is qualitatively similar to the latter case, but the pitchfork occurs at $T_0 = \infty$, i.e. all three solutions (with β real) exist for any period $T > 0$.

We remark that if the traveling waves described above have zero mean, we are dealing with a special case of the 2π-periodic N-soliton solutions described in [Cas78], namely

$$u(x,t) = 2\,\mathrm{Re}\left\{\sum_{l=1}^{N} \frac{2}{e^{i[x+t-x_l(t)]}-1}\right\},$$

where $\mathrm{Im}\{x_l(0)\} > 0$ and the $x_l(t)$ satisfy the system of differential equations

$$\frac{dx_l}{dt} = \sum_{\substack{m=1\\ m\neq l}}^{N} \frac{2}{e^{-i(x_m-x_l)}-1} + \sum_{m=1}^{N} \frac{2}{e^{-i(x_l-x_m^*)}-1}, \qquad (1\le l\le N). \tag{9}$$

In our notation, we write

$$x_l(t) = \overline{i\log\beta_l(t)} = \theta_l(t) - i\log|\beta_l(t)|, \qquad (\beta = |\beta|e^{-i\theta})$$

and generalize to the case that the mean α_0 can be non-zero. We find from (9) and (7) that $u(x,t) = \alpha_0 + \sum_l u_{\beta_l(t)}(x)$ is a solution of (1) if the variables $\beta_l \in \Delta$ satisfy

$$\dot\beta_l = \sum_{\substack{m=1\\ m\neq l}}^{N} \frac{2i}{\beta_l^{-1}-\beta_m^{-1}} + \sum_{m=1}^{N} \frac{2i\beta_l^2}{\beta_l-\bar\beta_m^{-1}} + i(1-\alpha_0)\beta_l, \qquad (1\le l\le N). \tag{10}$$

The N-hump traveling wave then has the representation

$$u_{\alpha_0,N,\beta}(x,t) = \alpha_0 + \sum_{l=1}^{N} u_{\beta_l(t)}(x), \qquad \beta_l(t) = \sqrt[N]{\beta}e^{-ict}, \qquad c = \alpha_0 - N\alpha(\beta),$$

where each β_l is assigned a distinct Nth root of β. As we are interested in developing numerical methods that generalize to more complicated systems such as the vortex sheet with surface tension and the water wave, we do not exploit the existence of soliton solutions in our numerical method; however, the non-trivial periodic solutions we find do turn out to be of this form; see Section 6.

3 Linear Theory

We formulate the problem of finding time-periodic solutions of the Benjamin-Ono equation as that of finding an initial condition u_0 and period T such that $F(u_0,T) = 0$, where $F : H^1 \times \mathbb{R} \to H^1$ is given by

$$F(u_0,T) = u(\cdot,T) - u_0, \qquad u_t = Hu_{xx} - uu_x, \quad u(\cdot,0) = u_0. \tag{11}$$

Clearly, stationary solutions are periodic with any period T. Although it is not strictly applicable due to a small divisor problem (discussed below), Liapunov-Schmidt theory

[GS85, Kie04] can help us predict which values of T will serve as bifurcation points for the equation $F(u_0, T) = 0$, and also tells us the dimension of the manifold of nearby non-trivial solutions and the symmetries we should expect these solutions to possess. We begin by linearizing the problem about the stationary solutions. Bifurcation from traveling waves can be reduced to this case by adding an appropriate constant and requiring that the period of the perturbation coincide with the period of the traveling wave (although there may be a phase shift involved as well); we present a detailed analysis of the traveling case in [AW].

3.1 Linearization About Stationary Solutions

Let $u = u_{N,\beta}$ be an arbitrary N-hump stationary solution. If $u(x) + v(x,t)$ is to satisfy (1) to first order in v, then v should satisfy

$$v_t = Hv_{xx} - (uv)_x. \tag{12}$$

(The exact solution satisfies $v_t = Hv_{xx} - (uv)_x - vv_x$). Equation (12) can be written

$$v_t = iBAv, \tag{13}$$

where the (unbounded, self-adjoint) operators A and B on H^1 are defined as

$$A = H\partial_x - u, \qquad B = \frac{1}{i}\partial_x. \tag{14}$$

To solve (13), we are interested in the eigenvalue problem

$$BAz = \omega z, \tag{15}$$

so that if BA has a complete set of eigenvectors, the general solution of (13) will be a superposition of functions of the form

$$v(x,t) = \mathrm{Re}\{Cz(x)e^{i\omega t}\}, \qquad C \in \mathbb{C}.$$

Of course, the eigenvalues of a composition of Hermitian operators need not be real, but for A and B in (14), we can compute all the eigenvalues explicitly, and they are indeed real. We do this numerically (which surprisingly leads us to formulas we can check analytically) by truncating the Fourier representations of A and B and computing the eigenvalues of the matrix $\hat{B}\hat{A}$. More precisely, we choose a cutoff frequency K (e.g. $K = 240$) and define the $(2K-1) \times (2K-1)$ matrices

$$\hat{A}_{kl} = |k|\delta_{kl} - \hat{u}_{k-l} = |k|\delta_{kl} - \overline{\hat{u}_{l-k}}, \qquad \hat{B}_{kl} = k\delta_{kl}, \qquad (-K < k, l < K), \tag{16}$$

where $\hat{u}_k$ was given in (6) and $\delta_{kl} = 1$ if $k = l$ and 0 otherwise. By carefully studying the eigenvalues for different values of N and $\beta = -\sqrt{(1-\alpha)/(3-\alpha)}$ with $\alpha < 1$, we determined that

$$\omega_{N,n} = \begin{cases} -\omega_{N,-n} & n < 0, \\ 0 & n = 0, \\ (n)(N-n) & 1 \le n \le N-1, \\ (n+1-N)\big(n+1+N(1-\alpha)\big) & n \ge N. \end{cases} \tag{17}$$

With this numbering, the first $N-1$ non-zero eigenvalues are independent of α:

$$\begin{array}{c|c} & n \\ \hline N & \omega_{N,n} \end{array} \quad = \quad \begin{array}{c|ccccccc} & 1 & 2 & 3 & 4 & 5 & 6 & \cdots \\ \hline 1 & * & * & * & * & * & * & \cdots \\ 2 & 1 & * & * & * & * & * & \cdots \\ 3 & 2 & 2 & * & * & * & * & \cdots \\ 4 & 3 & 4 & 3 & * & * & * & \cdots \\ 5 & 4 & 6 & 6 & 4 & * & * & \cdots \\ 6 & 5 & 8 & 9 & 8 & 5 & * & \cdots \end{array} \tag{18}$$

Note that $\omega_{N,N} = (2-\alpha)N + 1 \ge N+1$ and $\omega_{N,n}$ is strictly increasing in n for $n \ge N$, but $\omega_{N,N}$ could be less than $\omega_{N,\lfloor N/2 \rfloor}$ when $N \ge 6$ (and some of the eigenvalues can coalesce, increasing their multiplicity). Nevertheless, the ordering of the eigenvalues in (17) is more convenient than the monotonic ordering due to the fact that a pathway of non-trivial solutions connecting an N-hump traveling wave to an N'-hump traveling wave with $N < N'$ seems to involve $\omega_{N,n}$ and $\omega_{N',n'}$ with $n \ge N$ and $n' < N'$ satisfying $N' = n+1$ and $n' = N' - N$; see [AW].

The zero eigenvalue $\omega_{N,0} = 0$ has geometric multiplicity two and algebraic multiplicity three. The fact that the dimension of the kernel is independent of α indicates that there are no special values of the mean $N\alpha$ at which these N-hump stationary solutions bifurcate to more complicated stationary solutions. The two eigenfunctions in the kernel of BA are

$$z_{N,0}^{(1,0)}(x) = -u_x(x) = \frac{\partial}{\partial\theta}\bigg|_{\theta=0} u_{N,\beta}(x-\theta), \qquad z_{N,0}^{(2)}(x) = \frac{\partial}{\partial|\beta|} u_{N,\beta}(x), \tag{19}$$

which correspond to translating the stationary solution by a phase or decreasing its mean, $N\alpha = N(1-3|\beta|^2)/(1-|\beta|^2)$. There is also a Jordan chain [Wil07a] of length two associated with $z_{N,0}^{(1,0)}(x)$, namely

$$z_{N,0}^{(1,1)}(x) = i, \qquad \Big(BA z_{N,0}^{(1,1)} = z_{N,0}^{(1,0)}\Big). \tag{20}$$

The corresponding solution of (13) is

$$v(x,t) = -iz_{N,0}^{(1,1)}(x) + tz_{N,0}^{(1,0)}(x) = 1 - tu_x(x) = \frac{\partial}{\partial\varepsilon}\bigg|_{\varepsilon=0} [u(x-\varepsilon t) + \varepsilon],$$

i.e. this linear growth mode arises due to the fact that adding a constant to a stationary solution causes it to travel. The multiple eigenvalues $\omega_{N,n} = \omega_{N,N-n}$ with $1 \le n \le N-1$ pose a minor obstacle to obtaining explicit formulas for the eigenvectors. We eventually realized that because the shift operator

$$S_\theta z(x) = z(x-\theta), \qquad \hat{S}_{\theta,kl} = e^{-ik\theta}\delta_{kl}, \qquad \theta = 2\pi/N \tag{21}$$

commutes with BA, the eigenspaces of BA are invariant under the action of S_θ. Thus we can impose the additional requirement that if z is an eigenvector of BA corresponding to a multiple eigenvalue, then z should also satisfy

$$\hat{z}_k \neq 0 \quad \text{and} \quad \hat{z}_l \neq 0 \quad \Rightarrow \quad k - l \in N\mathbb{Z},$$

i.e. the non-zero Fourier coefficients are equally spaced with stride length N. Using this condition to make the eigenvectors unique up to scaling, we were able to recognize the patterns that emerge in the numerical eigenvectors (with the exception of the coefficient C and the $j = 0$ case when $n \ge N$, which we determined analytically):

$$\hat{z}_{N,n,k}\Big|_{k=n+jN} = \left\{ \begin{array}{cc} \left(1 + \frac{N(|j|-1)}{N-n}\right)\bar{\beta}^{|j|-1} & j < 0 \\ C\left(1 + \frac{Nj}{n}\right)\beta^{j+1} & j \ge 0 \end{array} \right\}, \qquad \left(\begin{array}{c} 1 \le n \le N-1 \\ C = \frac{-nN}{(N-n)\left[n+(N-n)|\beta|^2\right]} \end{array} \right),$$

$$\hat{z}_{N,n,k}\Big|_{k=n-N+1+jN} = \left\{ \begin{array}{cc} 0 & j < 0 \\ \frac{-\bar{\beta}}{(1-|\beta|^2)^2}\left[1 - \left(1 - \frac{N}{n+1}\right)|\beta|^2\right] & j = 0 \\ \left(1 + \frac{N(j-1)}{n+1}\right)\beta^{j-1} & j \ge 1 \end{array} \right\}, \qquad (n \ge N). \tag{22}$$

These formulas can be summed to obtain $z_{N,n}(x)$ as a rational function of e^{ix}, but we prefer to work with the Fourier coefficients. Note that as $n \to \infty$ (holding N fixed), the index $k = n - N + 1$ of the first non-zero Fourier mode increases to infinity. The eigenvectors corresponding to negative eigenvalues $\omega_{N,-n}$ with $n \ge 1$ satisfy $z_{N,-n}(x) = \overline{z_{N,n}(x)}$, so the Fourier coefficients appear in reverse order, conjugated: $\hat{z}_{N,-n,k} = \overline{\hat{z}_{N,n,-k}}$. When β is real, the Fourier coefficients are real and $z_{N,-n}(x) = z_{N,n}(-x)$. We have verified the formulas (17) and (22) analytically, and can also prove that the Fourier representation of these eigenvectors (together with the associated vector corresponding to the Jordan chain) form a Riesz basis for $\ell^2(\mathbb{Z})$; hence, we have not missed any eigenvalues.

3.2 Bifurcation from Stationary Solutions

Now that we have solved the eigenvalue problem for BA, we can compute the derivative of the operator F in (11) above. We continue to assume that u is an N-hump stationary

solution so that $DF = (D_1F, D_2F) : H^1 \times \mathbb{R} \to H^1$ satisfies

$$\begin{aligned} D_1F(u,T)v_0 &= \frac{\partial}{\partial\varepsilon}\Big|_{\varepsilon=0} F(u+\varepsilon v_0, T) = v(\cdot,T) - v_0 = \left[e^{iBAT} - I\right] v_0, \\ D_2F(u,T)\tau &= \frac{\partial}{\partial\varepsilon}\Big|_{\varepsilon=0} F(u, T+\varepsilon\tau) = 0. \end{aligned} \tag{23}$$

Note that $v_0 \in \ker D_1F(u,T)$ iff the solution $v(x,t)$ of the linearized problem is periodic with period T. As a result, a basis for the kernel of $DF(u,T)$ consists of $(0;1)$ together with all pairs $(v_0;0)$ of the form

$$v_0(x) = \mathrm{Re}\{z_{N,n}(x)\} \qquad \text{or} \qquad v_0(x) = \mathrm{Im}\{z_{N,n}(x)\}, \tag{24}$$

where n ranges over all integers such that

$$\omega_{N,n}T \in 2\pi\mathbb{Z}. \tag{25}$$

Negative values of n have already been accounted for in (24) using $z_{N,-n}(x) = \overline{z_{N,n}(x)}$, and the $n = 0$ case always yields two vectors in the kernel, namely those in (19). These directions do not cause bifurcations as they lead to other stationary solutions in the two parameter family. Thus, the periods at which bifurcations are expected are

$$T_{N,n,m} = \frac{2\pi m}{\omega_{N,n}}, \qquad (m,n \geq 1). \tag{26}$$

Note that this set is dense on the positive real line since $\omega_{N,n} \to \infty$ as $n \to \infty$. For a given T in this set, we would like to apply Liapunov-Schmidt theory [GS85, Kie04] to understand the bifurcation to non-trivial time periodic solutions. However, this would require that $DF(u,T)$ be a Fredholm operator, which fails in our case. Indeed, from (17), we see that if α is irrational, then although the kernel of $DF(u,T)$ is at most seven dimensional (see below), the values of $\left(e^{i\omega_n T} - 1\right)$ can be made arbitrarily small by choosing n appropriately; hence, the range of $D_1F(u,T)$ is not closed. And if $\alpha \in \mathbb{Q}$, there are infinitely many values of n such that (25) holds; hence the kernel of $DF(u,T)$ is infinite dimensional (but at least its range is closed).

In spite of this small divisor problem, it is instructive to consider what Liapunov-Schmidt theory would tell us if we ignore the illegal use of the implicit function theorem. After all, bifurcations from constant solutions to traveling waves also have a small divisor problem when formulated in terms of solving $F(u_0,T) = 0$, yet in this case we have exact formulas for the traveling waves (beyond the linearization), and they are consistent with the predictions of Liapunov-Schmidt theory. On the other hand, these traveling waves themselves bifurcate into non-trivial solutions at a dense set of bifurcation times, which means there are non-trivial time-periodic solutions arbitrarily close to the original constant solution. These

non-trivial solutions are presumably *not* predicted by Liapunov-Schmidt theory when we linearize about the constant solution. We believe the same situation occurs when bifurcating from stationary and traveling waves: Liapunov-Schmidt theory will correctly predict the existence, dimension and symmetries of a manifold of non-trivial solutions in a neighborhood of the stationary or traveling solution, but will not predict higher order bifurcations emanating from this manifold. Consistent with this claim, we have found one family of exact non-trivial solutions bifurcating from the one-hump stationary solution with all the expected properties; see Section 6.

We remark that small divisors can often be dealt with successfully using Nash-Moser theory; see e.g. [Nir01, PT01, IPT05]. This may be overkill, however, as it may be possible to get around the small divisor problem by working with the ODE governing soliton evolution but limiting the number of solitons that can be "created" by the bifurcation. It appears that the bifurcation corresponding to the eigenvalue $\omega_{N,n}$ with $n \geq N$ is an $(n+1)$-soliton solution. The origin in the unit disk in the β-plane can be thought of as an infinite source of new solitons $u_{\beta_l(t)}(x)$. Thus, by limiting the number of solitons, we eliminate the high frequency eigenvalues responsible for the small divisor problem.

We now briefly summarize the Liapunov-Schmidt reduction. As we use zero subscripts to denote initial conditions, we will use a tilde to denote a point around which we linearize. If $F : X \to Y$ is a sufficiently smooth mapping between Banach spaces satisfying $F(\tilde{x}) = 0$, and if $DF(\tilde{x})$ is a Fredholm operator, then we can decompose $X = \mathcal{N} \oplus \mathcal{N}'$ and $Y = \mathcal{R} \oplus \mathcal{R}'$ into direct sums, where $\mathcal{N} = \ker DF$, $\mathcal{R} = \operatorname{ran} DF$, and a prime denotes a complement of a subspace; (these complements exist because $\mathcal{N}$ is finite dimensional while $\mathcal{R}$ is closed and has finite codimension). The solution of $F(x) = 0$ for x near $\tilde{x}$ is then equivalent to the two equations

$$PF(x) = 0, \qquad (I - P)F(x) = 0, \tag{27}$$

where $P : Y \to \mathcal{R}$ is the projection along $\mathcal{R}'$ onto $\mathcal{R}$. Since the derivative of $w \mapsto PF(\tilde{x}+w)$ is an isomorphism from $\mathcal{N}'$ to $\mathcal{R}$ at $w = 0$, the implicit function theorem (applied to $f(v, w) = PF(\tilde{x}+v+w)$ at $v = 0$, $w = 0$) gives a mapping $W : \mathcal{N} \to \mathcal{N}'$ such that solutions of $PF(x) = 0$ for x near $\tilde{x}$ are precisely the vectors $x = \tilde{x} + v + W(v)$ with $v \in \mathcal{N}$ near zero. W is as smooth as F and satisfies $W(0) = 0$. So we have reduced the problem of solving $F(x) = 0$ to solving the finite dimensional system of equations

$$(I - P)F(\tilde{x} + v + W(v)) = 0, \tag{28}$$

where v ranges only over $\mathcal{N}$ near zero.

In our case, F was given in (11), $X = H^1 \times \mathbb{R}$, $Y = H^1$, and we linearize around an N-hump stationary solution $\tilde{u} = u_{N,\beta}$ at time $\tilde{T} = T_{N,n,m}$. We will assume β is real (so that

$\tilde{u}$, $z_0^{(2)}$, $\mathrm{Re}\{z_{N,n}\}$ and $\mathrm{Re}\{Az_{N,n}\}$ are even functions while $z_0^{(1,0)}$, $\mathrm{Im}\{z_{N,n}\}$ and $\mathrm{Im}\{Az_{N,n}\}$ are odd). We also assume α is irrational so that $\mathcal{N}$ is either 5 dimensional (if $\omega_{N,n}$ is a simple eigenvalue) or 7 dimensional (if $\omega_{N,n}$ is a double eigenvalue). In the former case, $\mathcal{N}$ is spanned by $(0;1)$ and $(v_0;0)$ with v_0 ranging over

$$z_0^{(1,0)}, \qquad z_0^{(2)}, \qquad \mathrm{Re}\{z_{N,n}\}, \qquad \mathrm{Im}\{z_{N,n}\}. \tag{29}$$

In the latter case, we also include $\mathrm{Re}\{z_{N,N-n}\}$ and $\mathrm{Im}\{z_{N,N-n}\}$ in the list. Meanwhile, the orthogonal complement $\mathcal{R}'$ of the range is either 4 dimensional or 6 dimensional, and is spanned by

$$\tilde{u}, \qquad 1, \qquad \mathrm{Re}\{Az_{N,n}\}, \qquad \mathrm{Im}\{Az_{N,n}\}, \tag{30}$$

together with $\mathrm{Re}\{Az_{N,N-n}\}$ and $\mathrm{Im}\{Az_{N,N-n}\}$ in the latter case. This follows from the fact that the adjoint of $DF = (e^{iBAT} - I, 0)$ is $DF^* = (e^{-iABT} - I; 0)$. Thus, (28) consists of 4 equations in 5 unknowns or 6 equations in 7 unknowns. However, some of these equations are redundant due to invariants and symmetries of the Benjamin-Ono equations. In particular, the equation corresponding to $1 \in \mathcal{R}'$ imposes the condition that the mean of $u(\cdot, T)$ should equal the mean of u_0, which is true of any solution of B-O. There are potentially two other redundancies in the equations arising from the fact that any periodic solution can be phase shifted in space and time to obtain other solutions; in the case of stationary solutions and traveling waves, the phase shift in time does not add anything new; but if the solution is genuinely time periodic, both phase shifts yield new solutions. (Constant solutions do not change under either operation).

Unfortunately, the Liapunov-Schmidt reduction does not respect the symmetry of the equations with respect to translation in space (as this would involve translating the underlying stationary solution, which is frozen in the linearization), so it is difficult to untangle the reduced equations to identify how they are redundant. However, we have noticed in our numerical simulations that all non-trivial time periodic solutions we are able to find have even symmetry (in space) at some time in their evolution, possibly after a spatial phase shift. This can be understood via the following symmetry argument. Let γ represent reflection about the origin, i.e.

$$\gamma u(x) = u(-x) = u(2\pi - x), \tag{31}$$

by periodicity. We slightly modify the definition of F in (11) via

$$F(u_0, T) = u(\cdot, T/2) - u(\cdot, -T/2), \qquad u_t = Hu_{xx} - uu_x, \quad u(\cdot, 0) = u_0. \tag{32}$$

Since $U(x,t) = u(-x,-t)$ is also a solution of Benjamin-Ono,

$$F(\gamma u_0, T) = -\gamma F(u_0, T), \qquad (u_0 \in H^1). \tag{33}$$

In the Liapunov-Schmidt reduction, γ leaves $\mathcal{N}$, $\mathcal{N}'$, $\mathcal{R}$ and $\mathcal{R}'$ invariant since each of the basis functions in (29) and (30) is even or odd; hence P commutes with γ and

$$0 = PF(\tilde{u} + \gamma v_0 + W(\gamma v_0, \tau), \tilde{T} + \tau) = -\gamma PF(\tilde{u} + v_0 + \gamma^{-1} W(\gamma v_0, \tau), \tilde{T} + \tau) \tag{34}$$

for all $(v_0, \tau) \in (\mathcal{N} \times \mathbb{R}) \cap B_\varepsilon(0,0)$, where $B_\varepsilon(0,0)$ is a small ball of radius ε. From the implicit function theorem, W is the unique function with this property, hence

$$\gamma^{-1} W(\gamma v_0, \tau) = W(v_0, \tau). \tag{35}$$

It follows that if v_0 is an even function, then so is $W(v_0, \tau)$. Thus, if we restrict attention to perturbations v_0 that are even functions when we solve the reduced equations

$$(I - P)F(\tilde{u} + v_0 + W(v_0, \tau), \tilde{T} + \tau) = 0, \qquad (v_0, \tau) \in \ker DF(\tilde{u}, \tilde{T}) \cap B_\varepsilon(0,0), \tag{36}$$

several of the equations will be satisfied automatically. Indeed, if v_0 is an even function, then $F(\tilde{u} + v_0 + W(v_0, \tau), \tilde{T} + \tau)$ will be an odd function and the components of the projection $I - P$ involving $\tilde{u}$, $\mathrm{Re}\{Az_{N,n}\}$ and, in the double eigenvalue case, $\mathrm{Re}\{Az_{N,N-n}\}$, will be zero automatically. As a result, instead of 3 equations in 5 unknowns or 5 equations in 7 unknowns, we are left with 1 equation in 3 unknowns or 2 equations in 4 unknowns, depending on the multiplicity of $\omega_{N,n}$. If we further restrict to solutions with a given mean α_0, the number of unknowns decreases by one and we finally have a bifurcation problem simple enough to thoroughly explore via numerical simulations.

This argument explains why we expect to find solutions of the reduced equations that possess even symmetry, but does not rule out the possibility that other solutions also exist. Indeed, other solutions do exist, for if we find an initial condition u_0 that yields a periodic solution, then a spatial phase shift $S_\theta u(\cdot, t_0)$ of any time slice would not in general be an even function, but would nevertheless satisfy $F(S_\theta u(\cdot, t_0), T) = 0$. The resulting manifold of solutions is four dimensional, with the mean, two phases and one essential bifurcation parameter describing the set of solutions. This manifold presumably also bifurcates at points arbitrarily close to the original stationary solution, but these additional solutions are presumably not predicted by Liapunov-Schmidt theory when linearizing about the stationary solution. We do not know if such interior bifurcations might break symmetry and yield solutions that cannot be phase-shifted to possess even symmetry at $t = 0$.

If α is irrational but $\omega_{N,n}$ is a double eigenvalue, we find (numerically) that there are two four-parameter sheets of solutions bifurcating from the stationary solution. One sheet corresponds to perturbing the stationary solution in the $\mathrm{Re}\{z_{N,n}(x)\}$ direction and the other corresponds to moving in the $\mathrm{Re}\{z_{N,N-n}(x)\}$ direction. Similarly, when α is rational, although the kernel of $DF(\tilde{u}, T)$ is now infinite dimensional, the modes seem to bifurcate

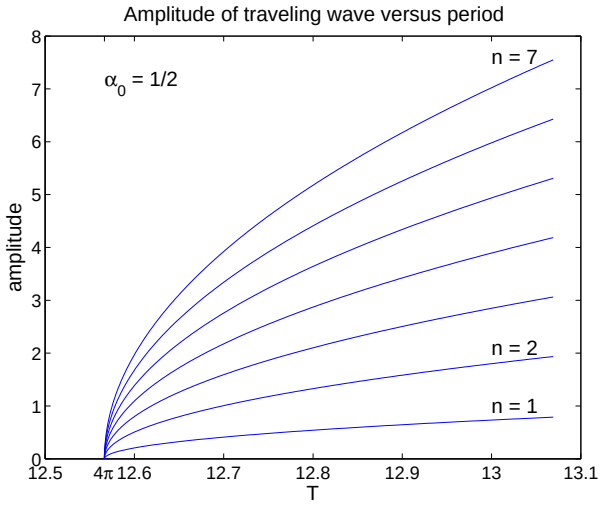

Figure 2: First seven bifurcations from the constant solution $\tilde{u}(x) = \alpha_0$ to traveling waves with n-humps. The period shown is $T = 2\pi m/[n(n\alpha - \alpha_0)]$ with $m = 2n(n - 1/2)$. We used this to solve for $|\beta|$ in terms of T via (3). The amplitude shown is the difference between the maximum and minimum values of the solution, i.e. $8n|\beta|/(1 - |\beta|^2)$.

independently, each in the same fashion as described above for the irrational case. We observe an analogous phenomenon when bifurcating from constant solutions to traveling waves; see Figure 2. When $\tilde{u} = \alpha_0$ is a constant function, $\hat{A}$ and $\hat{B}$ are both diagonal matrices, the eigenvalues and eigenvectors of BA are given by

$$\omega_n = n(|n| - \alpha_0), \qquad z_n(x) = e^{inx}, \qquad (n \in \mathbb{Z}),$$

and the bifurcation times are given by

$$T_{n,m} = 2\pi m/(n|\alpha_0 - n|), \qquad (n, m \geq 1).$$

Note that in this simplified problem, the bifurcation index n turns out to be the number of humps. If $\alpha_0 = 1/2$ and $T = 4\pi$, then $\omega_n T \in 2\pi\mathbb{Z}$ for *every* n, i.e. the kernel $\mathcal{N}$ of $DF(\tilde{u}, T)$ is the whole space H^1. Nevertheless, the traveling solutions that emerge from this bifurcation are no different than if α_0 were irrational – they all just happen to join together at $T = 4\pi$. More specifically, the n-hump traveling solutions $u_{\alpha_0,n,\beta}(x,t)$ defined in (8) above have the property that as $\beta \to 0$ (and hence $\alpha \to 1$), a multiple m of their shortest period $2\pi/[n(n\alpha - \alpha_0)]$ converges to 4π.

4 The Method

In order to compute non-trivial time periodic solutions, we define the functional

$$G_{\text{tot}}(u_0, T) = G(u_0, T) + \varphi(u_0, T) \tag{37}$$

with

$$G(u_0, T) = \frac{1}{2}\int_0^{2\pi} [u(x, T) - u_0(x)]^2 \, dx \tag{38}$$

and look for minimizers of G_{tot} with the hope that the minimum value will be zero. Here $\varphi(u_0, T)$ is a non-negative penalty function designed to eliminate the two phase-shift degrees of freedom and specify the mean and the value of the essential bifurcation parameter. Our first goal is to find an efficient method of computing the variational derivative of G. As usual in optimal control problems [Pir84], there is an adjoint PDE that allows us to compute $\frac{\delta G}{\delta u_0}$ in as little time as it takes to compute G itself. We will then use a spectral method in space and a fourth order semi-implicit Runge-Kutta method [CS83, KC03, Wil07b] in time to solve the Benjamin-Ono and adjoint equations to compute G, $\frac{\delta G}{\delta u_0}$ and $\frac{\partial G}{\partial T}$ in the inner loop of the BFGS minimization algorithm [Bro70, NW99].

4.1 Variational Derivative of G

Let u_0 be any function in H^1 (not necessarily leading to a periodic solution). Evidently,

$$\frac{\partial}{\partial T} G(u_0, T) = \int_0^{2\pi} [u(x, T) - u_0(x)] u_t(x, T) \, dx. \tag{39}$$

Let $v_0 \in H^1$ be given and define $\dot{G} = D_1 G(u_0, T) v_0$, i.e.

$$\dot{G} = \frac{d}{d\varepsilon}\Big|_{\varepsilon=0} G(u_0 + \varepsilon v_0, T) = \int_0^{2\pi} [u(x, T) - u_0(x)][v(x, T) - v_0(x)] \, dx. \tag{40}$$

Here $v(x, t) = \dot{u}(x, t) = \frac{d}{d\varepsilon}\big|_{\varepsilon=0} u(x, t, \varepsilon)$ with $u(x, t, \varepsilon)$ the solution of Benjamin-Ono with initial condition $u(x, 0, \varepsilon) = u_0(x) + \varepsilon v_0(x)$. We can compute v by solving the variational equation

$$v_t = H v_{xx} - (uv)_x, \qquad v(x, 0) = v_0(x), \tag{41}$$

which is linear but non-autonomous (as u depends on time in general). Our next task is to eliminate $v(x, T)$ from (40) and represent $\dot{G}$ as an inner product:

$$\dot{G} = \int_0^{2\pi} \frac{\delta G}{\delta u_0}(x) \, v_0(x) \, dx. \tag{42}$$

The idea is to define a function $w(x, s)$ going backward in time (with $s = T - t$) such that

$$w(x, 0) = w_0(x) = u(x, T) - u_0(x) \tag{43}$$

and then determine how w should evolve so that

$$\int_0^{2\pi} w(x,0)v(x,T)\,dx = \int_0^{2\pi} w(x,T)v(x,0)\,dx. \tag{44}$$

Let us define the solution operator $V(t_2,t_1) : H^1 \to H^1$ for the linearized equation (41) as the mapping that evolves an initial condition specified at time t_1 to the solution at time t_2. These operators satisfy a non-autonomous, time reversible version of familiar semigroup properties:

$$V(t_1,t_1) = I, \qquad V(t_3,t_1) = V(t_3,t_2)V(t_2,t_1), \qquad (t_1,t_2,t_3 \in \mathbb{R}). \tag{45}$$

Equation (44) may now be written

$$\langle w_0, V(T,0)v_0\rangle = \langle W(T,0)w_0, v_0\rangle \tag{46}$$

where $\langle\cdot,\cdot\rangle$ is the L^2 inner product and we define $W(s_2,s_1) = V(t_1,t_2)^*$ with $t_j = T - s_j$. It follows from (45) that $W(s_1,s_1) = I$ and $W(s_3,s_1) = W(s_3,s_2)W(s_2,s_1)$. What remains is to determine how this non-autonomous semigroup W is generated. Taking the inner product of v_t with w, we have

$$\begin{aligned}\int v_t(x,t)w(x,s)\,dx &= \lim_{h\to 0}\int \left(\left[\frac{V(t+h,t)-V(t,t)}{h}\right]v(x,t)\right)w(x,s-h)\,dx \\ &= \lim_{h\to 0}\int v(x,t)\left(\left[\frac{W(s,s-h)-I}{h}\right]w(x,s-h)\right)\,dx = \int v(x,t)w_s(x,s)\,dx. \end{aligned}\tag{47}$$

We learn that

$$\int vw_s\,dx = \int v_t w\,dx = \int [Hv_{xx} - (uv)_x]w\,dx = \int v[-Hw_{xx} + uw_x]\,dx, \tag{48}$$

i.e. w should solve the adjoint equation to (41), namely

$$w_s(x,s) = -Hw_{xx}(x,s) + u(x,T-s)w_x(x,s). \tag{49}$$

The time reversal in the inhomogeneous term $u(x,T-s)$ is significant. Combining this with (40) and (42), we conclude that

$$\frac{\delta G}{\delta u_0}(x) = w(x,T) - w_0(x), \tag{50}$$

where w solves (49) with initial condition (43).

Remark: We emphasize that the steps we have just followed for the Benjamin-Ono equation can in principle be carried out for any PDE. These steps are simply:

1. Find the variational equation analogous to (12)

2. Find the appropriate adjoint equation, accounting for time-reversal.

The details of the initial condition of the adjoint problem and the formula for $\frac{\delta G}{\delta u_0}$ depend on the particular functional G we choose, but they are usually straightforward to work out. For example, as another variant, we could define

$$G(u_0, T) = \frac{1}{2}\int_0^{2\pi} [u(x, T/2) - u(2\pi - x, T/2)]^2 \, dx \tag{51}$$

to impose even symmetry at the half-way point. (Recall that if u_0 is symmetric, then $u(2\pi - x, T/2) = u(x, -T/2)$). In this case we find that

$$\frac{\delta G}{\delta u_0}(x) = 2w(x, T/2), \qquad w_0(x) = u(x, T/2) - u(2\pi - x, T/2), \tag{52}$$

or, since v_0 is assumed symmetric in this formulation, $\frac{\delta G}{\delta u_0}(x) = w(x, T/2) + w(2\pi - x, T/2)$. In subsequent work, we will apply the methods of this paper to the vortex sheet with surface tension and to the water wave.

4.2 The Numerical Method

We minimize G_{tot} using the BFGS algorithm [NW99], which is a quasi-Newton line search method that builds an approximate Hessian incrementally from the history of gradients it has evaluated. As a black box unconstrained minimization algorithm, it requires only an initial guess and subroutines to compute $G_{\text{tot}}(q)$ and $\nabla_q G_{\text{tot}}(q)$, where $q \in \mathbb{R}^d$ contains the numerical degrees of freedom used to represent u_0 and T. We use a stationary or traveling wave solution for the initial guess at a bifurcation point, and then use linear extrapolation (or the result of the previous iteration) for the initial guess in subsequent calculations as we vary the bifurcation parameter.

In our implementation, we wrote a C++ wrapper around J. Nocedal's L-BFGS Fortran code released in 1990, but we turn off the limited memory aspect of the code since computing G takes more time than the linear algebra associated with updating the full Hessian matrix. We do find that the algorithm converges quadratically once it gets close to a minimizer. Our code also makes use of the FFTW and LAPACK libraries, but was otherwise written from scratch.

We represent $u(x, t)$ spectrally as a sum of M (typically 384 or 512) Fourier modes,

$$u(x, t) = \sum_{k=-M/2+1}^{M/2} c_k(t) e^{ikx}, \qquad c_k \in \mathbb{C}. \tag{53}$$

Since u is real, we use the r2c version of the FFT algorithm, which only accesses the coefficients c_k with $k \geq 0$, assuming $c_{-k} = \bar{c}_k$. We also zero out the Nyquist frequency $c_{M/2}$

so that the total number of (real) degrees of freedom representing u at time t is $M-1$. We use $d = M/2$ degrees of freedom to represent u_0 and T, namely

$$q = (a_0, T, a_1, b_1, \ldots, a_{M/4-1}, b_{M/4-1}) \in \mathbb{R}^d, \qquad (c_k = a_k + ib_k,\ t = 0). \tag{54}$$

The remaining Fourier modes in u_0 are taken to be zero. The reason for using fewer Fourier modes in the initial condition is that in order to avoid aliasing errors, we want the upper half of the spectrum to remain close to zero throughout the calculation; therefore, we do not wish to give BFGS the opportunity to modify these coefficients. We increase M and repeat the calculation any time one of the high frequency ($k \geq M/4$) Fourier modes of the optimal solution exceeds 10^{-13} in magnitude at any timestep.

To compute $G(q)$, we write the Benjamin-Ono equation in the form

$$u_t = f(u) + g(u), \qquad g(u) = Hu_{xx}, \quad f(u) = -\left(\tfrac{1}{2}u^2\right)_x, \tag{55}$$

where $\frac{1}{2}u^2$ is evaluated on the grid $\{x_j = 2\pi j/M \ :\ 0 \leq j \leq M-1\}$ in physical space while H and ∂_x are evaluated in Fourier space. The trapezoidal rule in physical space is used to evaluate the integral (38) defining G. To evolve the solution, we use the stiffly stable, additive (i.e. implicit-explicit) Runge-Kutta method of Kennedy and Carpenter [KC03, Wil07b] known as ARK4(3)6L[2]SA with a fixed timestep $h = T/N$, where N is chosen to be large enough that further refinement does not improve the solution. Briefly, the idea of an ARK method is to treat f explicitly (as it is non-linear) while treating g implicitly (as it is the source of stiffness):

$$\begin{aligned}
k_i &= f\left(t_n + c_i h,\, u_n + h\textstyle\sum_j a_{ij}k_j + h\sum_j \hat{a}_{ij}\ell_j\right), \\
\ell_i &= g\left(t_n + \hat{c}_i h,\, u_n + h\textstyle\sum_j a_{ij}k_j + h\sum_j \hat{a}_{ij}\ell_j\right), \\
u_{n+1} &= u_n + h\textstyle\sum_j b_j k_j + h\sum_j \hat{b}_j \ell_j.
\end{aligned} \qquad \begin{array}{c|c} c & A \\ \hline & b^T \end{array} \quad \text{for } f \qquad \begin{array}{c|c} \hat{c} & \hat{A} \\ \hline & \hat{b}^T \end{array} \quad \text{for } g \tag{56}$$

The Butcher array for f satisfies $a_{ij} = 0$ if $i \leq j$ and for g satisfies $\hat{a}_{ij} = 0$ if $i < j$, which allows the stage derivatives to be solved for in order: ℓ_1, k_1, ℓ_2, k_2, …, ℓ_6, k_6, where our scheme has 6 stages. See [KC03] for the scheme coefficients and [Wil07b] for details on solving the implicit equations in the similar cases of Burgers' equation and the KdV equation.

Once $u(x,T)$ is known, we use the same scheme to solve the adjoint equation

$$w_s = f(s,w) + g(w), \qquad g(w) = -Hw_{xx}, \qquad f(s,w)(x) = u(x, T-s)w_x(x). \tag{57}$$

The main difficulty is that the intermediate stages of the ARK method require the value of u at intermediate times (between timesteps). For this we use cubic Hermite interpolation,

matching u and u_t at the timesteps straddling the required intermediate time:

$$u(\cdot, t_n + \theta h) = (1-\theta)u_n + \theta u_{n+1} - \theta(1-\theta)\big[(1-2\theta)(u_{n+1}-u_n) - (1-\theta)h\partial_t u_n + \theta h \partial_t u_{n+1}\big]$$

where $0 < \theta < 1$. This yields fourth order accurate values of u in the right hand side of (57), which is sufficient to achieve a fourth order accurate global solution w. We include the option in our code to store u only at certain milemarker times, and then regenerate the data at all timesteps between milemarkers as soon as the w equation enters that region; this dramatically reduces the memory requirements of the code at the expense of having to compute u twice.

Once $u(x,T)$ and $w(x,T)$ are known with the appropriate initial conditions and period specified in $q \in \mathbb{R}^d$, we compute $G(q)$ using the trapezoidal rule in physical space to evaluate the integral in (38), and we compute $\frac{\partial G}{\partial q_j}$ by taking the FFT of $\frac{\delta G}{\delta u_0}$ and scaling each component appropriately:

$$\begin{aligned}
\frac{\partial G}{\partial q_0} &= \int_0^{2\pi} \frac{\delta G}{\delta u_0}(x)\, 1\, dx = 2\pi \left(\tfrac{\delta G}{\delta u_0}\right)^\wedge_0 \\
\frac{\partial G}{\partial q_1} &= \frac{\partial G}{\partial T} = \int_0^{2\pi} [u(x,T) - u_0(x)] u_t(x,T)\, dx, \quad \longleftarrow \quad \begin{pmatrix} \text{use trap. rule} \\ \text{in physical space} \end{pmatrix} \\
\frac{\partial G}{\partial q_{2k}} &= \frac{\partial G}{\partial a_k} = \int_0^{2\pi} \frac{\delta G}{\delta u_0}(x) \left(e^{ikx} + e^{-ikx}\right) dx = 4\pi\, \mathrm{Re}\left\{ \left(\tfrac{\delta G}{\delta u_0}\right)^\wedge_k \right\}, \qquad (k \geq 1), \\
\frac{\partial G}{\partial q_{2k+1}} &= \frac{\partial G}{\partial b_k} = \int_0^{2\pi} \frac{\delta G}{\delta u_0}(x) \left(ie^{ikx} - ie^{-ikx}\right) dx = 4\pi\, \mathrm{Im}\left\{ \left(\tfrac{\delta G}{\delta u_0}\right)^\wedge_k \right\}, \qquad (k \geq 1).
\end{aligned} \tag{58}$$

We remark that these formulas for the derivatives of the numerical version of G essentially assume that we have solved the PDE's exactly (so that the calculus of variations applies to our numerical solutions). This is reasonable in our case as we are using spectrally accurate schemes, but would cause difficulties if the numerical solution were only first or second order accurate in space or time.

4.3 Choice of Penalty Function φ

We still need to define the penalty function $\varphi(u_0, T)$ in (37) and show how to compute its gradient with respect to q. The purpose of φ is to pin down the mean and the phase shifts in space and time as well as to specify the bifurcation parameter. We have explored several successful variants which became more specialized as our understanding of the problem increased. As some of these variants may prove useful in other problems, we describe them here.

Initially we did not include a penalty function in G_{tot}, but without it, the BFGS algorithm invariably converges to a constant solution. Next we constrained q_2, the real part of

the first Fourier mode $\hat{u}_1(t) = a_1(t) + ib_1(t)$ at $t = 0$, to have a given value σ. We reasoned that as long as σ is not too large, the BFGS algorithm can vary $q_3 = b_1(0)$ to find a periodic solution, so all we are doing is pinning down a phase. This was done by defining

$$\varphi(u_0, T) = \frac{1}{2}\Big([a_0(0) - \alpha_0]^2 + [a_1(0) - \sigma]^2\Big) \qquad \text{or} \qquad \varphi(q) = \frac{1}{2}\Big([q_0 - \alpha_0]^2 + [q_2 - \sigma]^2\Big),$$

which works well to rule out the constant solutions but generally leads to traveling waves. By studying these traveling waves, we determined the formulas of Section 2 and also observed that for some choices of σ and starting guess $q^{(0)}$, the wave becomes "wobbly," indicating that a non-trivial solution might be nearby.

To rule out traveling waves, we chose a parameter $\eta \in [-1, 1]$ and defined

$$\varphi(u_0, T) = \frac{1}{2}\Big([a_0(0) - \alpha_0]^2 + [a_1(0) - \sigma]^2 + [a_1(T/2) - \eta a_1(0)]^2 + [b_1(T/2) - \eta b_1(0)]^2\Big).$$

Our idea here was that a (one-hump) traveling wave would have $\eta = \pm 1$, depending on how many times it passed through the domain in time T; hence, intermediate values of η would have to correspond to non-trivial solutions. To compute the gradient of φ when it involves Fourier modes at later times, we simply solve another adjoint problem. Specifically, if φ involves one of

$$a_k(T/2) = \frac{1}{2\pi}\int_0^{2\pi} u(x, T/2)\cos(kx)\,dx, \qquad b_k(T/2) = \frac{1}{2\pi}\int_0^{2\pi} u(x, T/2)[-\sin(kx)]\,dx,$$

we will need to compute $\frac{\delta}{\delta u_0} a_k(T/2)$ or $\frac{\delta}{\delta u_0} b_k(T/2)$, which can be done by setting

$$w_0(x) = \frac{1}{2\pi}\cos(kx), \qquad \text{or} \qquad w_0(x) = -\frac{1}{2\pi}\sin(kx)$$

and solving (49) from $s = 0$ to $s = T/2$; the result $w(x, T/2)$ is the desired variational derivative. These may then be used to compute $\frac{\partial}{\partial q_j} a_k(T/2)$ or $\frac{\partial}{\partial q_j} b_k(T/2)$ as was done for G in (58), at which point it is a simple matter to obtain $\frac{\partial \varphi}{\partial q_j}$.

This procedure proved very effective in obtaining non-trivial time periodic solutions. The BFGS algorithm is able to minimize G_{tot} down to 10^{-26}, at which point roundoff error prevents further reduction. With random initial data $q^{(0)}$, the algorithm explores quite a wide region of the parameter space, with all components of q (including T) changing substantially — we do not seem to get stuck in non-zero local minima of G_{tot}. Once we do find a nontrivial solution, varying η leads to other nearby periodic solutions.

Studying this family of solutions, we finally realized that we were dealing with a four parameter family of nontrivial solutions with the mean, two phases and a bifurcation parameter describing them. The main drawback of using η as the bifurcation parameter is

that the phases of the resulting solutions are by no means canonically specified. A more natural choice is to define

$$\varphi(u_0, T) = \frac{1}{2}\Big([a_0(0) - \alpha_0]^2 + [a_k(0) - \sigma]^2 + [b_k(0)]^2 + [\partial_t a_k(0)]^2\Big), \tag{59}$$

i.e. we use φ to impose the mean α_0, the bifurcation parameter σ, the spatial phase $b_k(0) = 0$, and the temporal phase $\partial_t a_k(0) = 0$. Given any solution, we can always translate space and time to achieve the latter two conditions – we have not made any symmetry assumptions here. The index k we use depends on the number of humps N and bifurcation index n of the linearized solution; the only requirement is that $\hat{z}_{N,n,k}$ in (22) be non-zero. One readily checks that

$$\partial_t a_k(0) = \frac{1}{2\pi}\int_0^{2\pi} u_t(x,0)\cos kx\,dx = \frac{1}{2\pi}\int_0^{2\pi}\left[-k^2 u_0 + (k/2)u_0^2\right](-\sin kx)\,dx, \tag{60}$$

from which we obtain $\frac{\delta}{\delta u_0}[\partial_t a_k(0)](x) = \frac{1}{2\pi}(k^2 - k u_0(x))\sin kx$. Although (59) does not rule out traveling waves, we have no difficulty bifurcating from traveling waves to non-trivial solutions by choosing a starting guess that includes first order corrections from the linear theory of Section 3.

We conclude this section by mentioning that we were at first surprised to see that all the non-trivial solutions we are able to find possess even spatial symmetry after an appropriate phase shift in space and time. The final choice of φ in (59) shifts the phases so that this even solution occurs at $t = 0$, but does not rule out the possibility of finding other types of periodic solutions. We developed the symmetry argument in Equation (33) to explain this numerical observation. Once it is known that one only needs to search for initial conditions u_0 with even symmetry, the most efficient and accurate numerical method would be to define G as in (51) and drop the last two terms in (59). By the time we understood this, we had already computed the bifurcation diagram in Figure 6 below; however, the simulations we report in the follow-up paper [AW] were performed using the symmetric version of the algorithm.

5 Non-Trivial Time-Periodic Solutions

We now use the methods described above to study the global behavior of non-trivial time-periodic solutions far beyond the realm of validity of the linearization about stationary and traveling waves. We find that these non-trivial solutions act as rungs in a ladder, connecting stationary and traveling solutions with different speeds and wavelengths by creating or annihilating oscillatory humps that grow or shrink in amplitude until they become part of

the stationary or traveling wave on the other side of the rung. The dynamics of these non-trivial solutions are often very interesting, sometimes looking like a low amplitude traveling wave superimposed on a lower frequency carrier signal, and other times looking like two bouncing solitons that repel each other to avoid coalescing. In this section, we present a detailed numerical study of the path of non-trivial solutions connecting the one-hump stationary solution to the two-hump traveling wave. In Section 6, we derive exact formulas for the solutions on this path. In a follow-up paper [AW], we classify all bifurcations from traveling waves, study the paths of non-trivial solutions connecting several of them, and propose a conjecture explaining how they all fit together.

Consider the periodic solutions obtained by bifurcating from a one-hump stationary solution at the lowest frequency, $\omega_{1,1}$. We arbitrarily set the mean $\alpha_0 = 0.544375$ for these simulations (see Figure 1 above), but as shown in Section 6, any choice of $\alpha_0 < 1$ would lead to similar results. In the top pane of Figure 3, we show the one-hump stationary solution $u_{1,\beta}(x)$ with $\beta = -\sqrt{(1-\alpha_0)/(3-\alpha_0)}$ together with the (initial conditions of the) two periodic solutions

$$v^{(0)}(x,t) = \mathrm{Re}\{z_{1,1}(x)e^{i\omega_1 t}\}, \qquad v^{(1)}(x,t) = \mathrm{Im}\{z_{1,1}(x)e^{i\omega_1 t}\} \tag{61}$$

of the linearized equation $v_t = Hv_{xx} - (uv)_x$ corresponding to the first eigenvalue $\omega_{1,1} = 3 - \alpha_0$ of $BA = -i\partial_x(H\partial_x - u)$. The natural period of these solutions is $T = 2\pi/\omega_{1,1} = 2.55869$. Note how the non-linearity of Benjamin-Ono distorts these two-hump perturbations as they travel (to the left) on top of the one-hump stationary "carrier" solution. Also note that $v^{(0)}$ and $v^{(1)}$ are actually the same solution with a $T/4$ phase lag in time:

$$v^{(0)}(x,T/4) = -v^{(1)}(x,0) \quad \text{while} \quad v^{(1)}(x,T/4) = v^{(0)}(x,0).$$

We choose the real part of the first Fourier mode as the bifurcation parameter σ so that $k = 1$ in the definition (59) of φ. As we vary $\sigma = a_1(0)$ from $-2\sqrt{(1-\alpha_0)/(3-\alpha_0)}$ to 0, we traverse the trajectory from B to F in the bifurcation diagram of Figure 4. The curves corresponding to the intermediate points H0, J0 and K0 along this path are shown in black in panes 2–4 of Figure 3. Along this path, we see that a second hump forms at $x = 0$ while the center hump sharpens to accommodate the shorter wavelength of the two-hump traveling wave. If we instead increase $|\sigma|$ near point B in the diagram, we obtain the lower path connecting B to G. Along this path, the center hump decreases in magnitude (curve H5), forms a dimple in the middle (curve J10), splits into two humps (curve K10), and again turns into a two-hump traveling wave (curve G). These curves are related to those on the path from B to F by a $T/2$ phase shift in time. If we change the sign of β (i.e. shift the phase by π) in the stationary solution and call the resulting curve C, the bifurcation

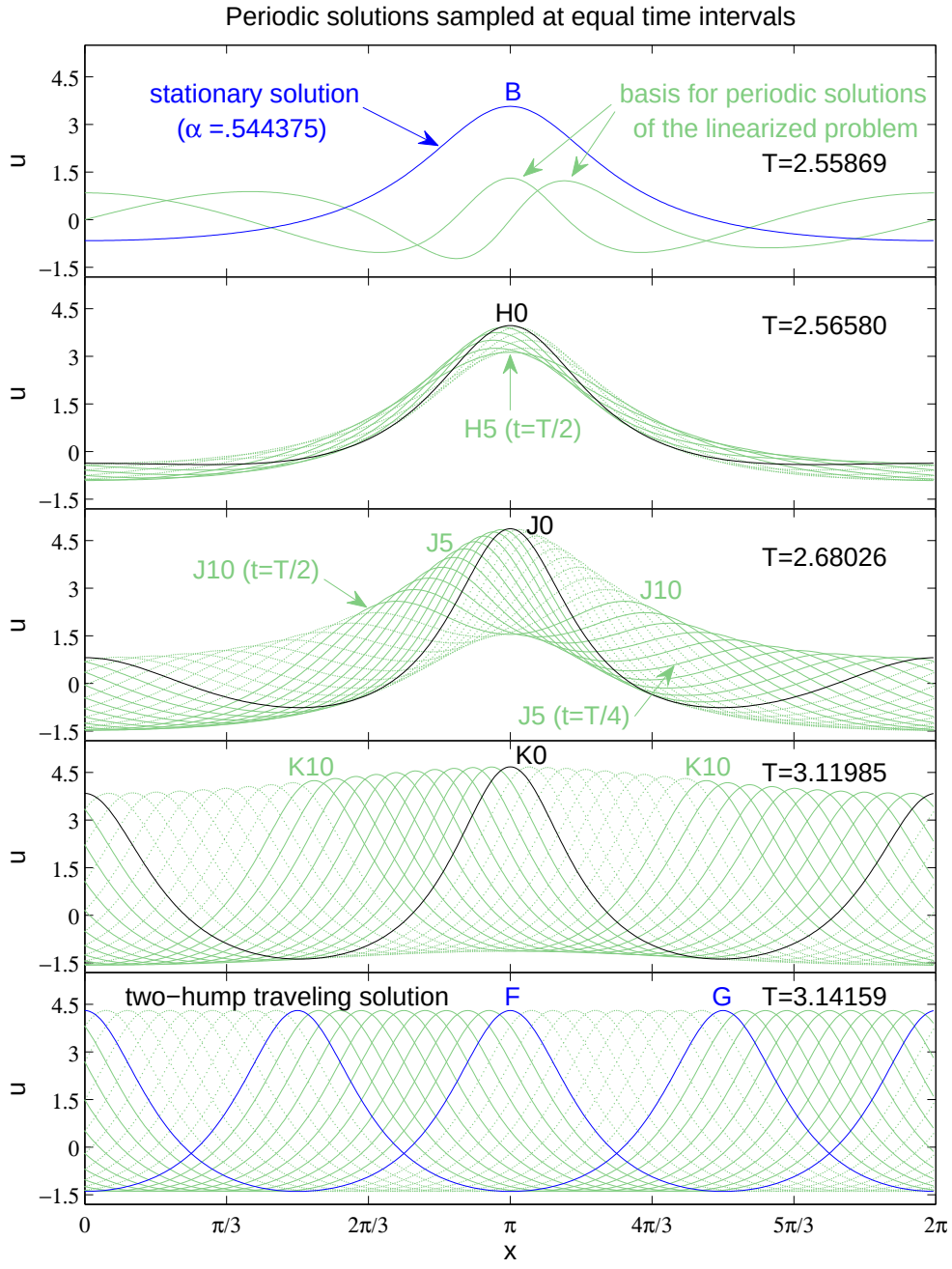

Figure 3: Progression from a one-hump stationary solution (top) to a two-hump traveling wave (bottom, moving left) by varying the real part of the first Fourier mode at $t = 0$ while holding the mean α_0 constant and choosing canonical spatial and temporal phases. The labels B, F, G, H0, J0, etc. correspond to Figures 4–8.

diagram is reflected about the T axis. The path from B (or C) to F is easier to compute due to the turning point in $|\sigma|$ on the path from B (or C) to G.

By the time we reach $K0$ on the path from B to F, we can view our solution as a two-hump traveling wave with a small one-hump stationary perturbation corresponding to the first eigenvalue $\omega_{2,1} = 1$ in the linearization about the two-hump traveling wave. A full analysis of the linearization about traveling waves is given in the follow-up paper [AW], but the idea is that if $u(x)$ is a stationary solution and $U(x,t) = u(x-ct)+c$ is a traveling wave, then the solutions v and V of the linearizations about u and U satisfy $V(x,t) = v(x-ct,t)$. Now, the linearized solutions $\mathrm{Re}\{z_{2,1}(x)e^{i\omega_{2,1}t}\}$ and $\mathrm{Im}\{z_{2,1}(x)e^{i\omega_{2,1}t}\}$ about the two-hump *stationary* solution have the property that $z_{2,1}(x-\pi) = -z_{2,1}(x)$; hence, when they are used as perturbations on a two-hump *traveling* wave, they need to progress through an extra half-cycle in time to make up for the sign change. As a result, $\omega_{2,1}T$ must belong to $\pi + 2\pi\mathbb{Z}$ (rather than $2\pi\mathbb{Z}$ itself) for the linearized solution to be periodic. It turns out that as we traverse the path from B to F, the period of the solution increases from $T = 2\pi/\omega_{1,1}$ up to $T = \pi/\omega_{2,1} = \pi$ (rather than e.g. 3π or 5π). Note that as $\omega_{2,1} = 1$ is independent of α_0, the path connecting the one hump stationary solution to the two-hump traveling wave always terminates at $T = \pi$, regardless of the mean.

In Figure 5, we plot the trajectories of the first Fourier mode $c_1(t) = a_1(t)+ib_1(t)$ in the complex plane for various choices of the bifurcation parameter $\sigma = a_1(0)$. We were surprised to find that these trajectories are exactly circular; this will be discussed further below. The markers on the left (west) lobe of circles correspond to solutions plotted in Figure 3; for example, J19 corresponds to $u\left(x, \frac{19}{20}T\right)$, which is the dotted curve immediately to the right of the initial condition J0 in the center pane of Figure 3. For visibility, we only plotted 10 timeslices in the evolution of H0.

The four parameter family of non-trivial solutions can be seen in Figure 5. A given solution is represented by one of the circular trajectories. The two main parameters describing this family are the mean α_0 and the distance from the nearest point on the circle to the origin. A spatial phase shift of the initial condition by θ (with the sign convention of Eq. (21)) amounts to a clockwise rotation of the circle about the origin by θ (or $k\theta$ for the kth Fourier mode). The north, east and south lobes of circles represent spatial phase shifts of the west lobe of solutions by $\theta = \pi/2$, π and $-\pi/2$, respectively, but any other phase shift $\theta \in \mathbb{R}$ is also allowed. Finally, a temporal phase shift amounts to choosing which point on the circle we assign to $t = 0$. Requiring that the initial condition have even symmetry yields either the west or east lobe of solutions with $t = 0$ occurring along the real axis.

We can also use other Fourier modes for the bifurcation parameter. This is especially important to track higher order bifurcations from multi-hump traveling waves — in these

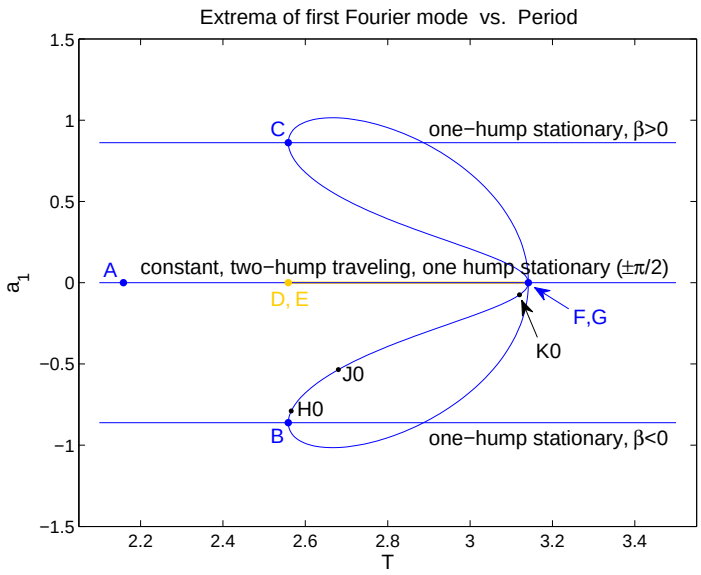

Figure 4: Bifurcation from one-hump stationary solutions (B and C) to non-trivial time-periodic solutions that re-connect with two-hump traveling waves at F and G.

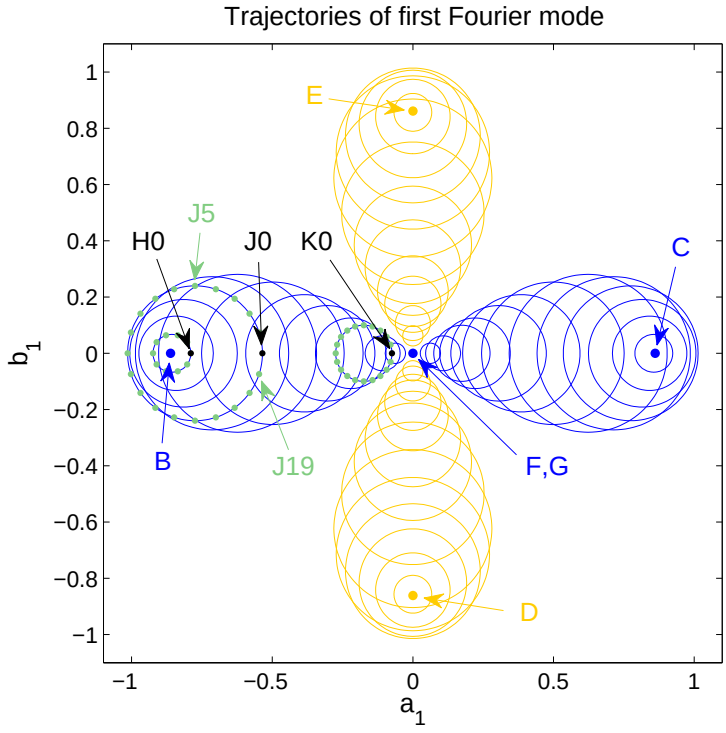

Figure 5: The trajectories of the first Fourier mode in the complex plane are exactly circular. The markers on the left lobe correspond to the solutions shown in Figure 3.

cases, the first several Fourier modes remain zero for all solutions in the family at all times t. But even for the simplest path connecting one-hump stationary solutions to two-hump traveling waves, it is useful to study other bifurcation diagrams representing this same family of solutions. In Figure 6, we show the result when the second Fourier mode is used instead of the first. By setting $\sigma = a_2(0)$, we can now also see the bifurcation (labeled A) from the constant solution $u \equiv \alpha_0$ to the two-hump traveling waves; moreover, the points F and G that fell on top of each other in Figure 4 become distinct. The outer curve connecting F to G via A represents the set of two-hump traveling waves moving left with mean α_0. This curve was plotted parametrically, setting $a_2 = \pm 2N\sqrt{(1-\alpha)/(3-\alpha)}$ and $T = 2\pi/[N(N\alpha - \alpha_0)]$ with $N = 2$ and α ranging over all values such that $\alpha \leq 1$ and $T \leq 3.5$.

It is interesting to note that the bifurcation at F (and at G) from the two-hump traveling wave to the path of non-trivial solutions does not look like a pitchfork in this case. Instead, the bifurcation curve enters at an oblique angle from one side only. This is because the second Fourier mode of the linearized solution $v^{(0)}(x,t) = \mathrm{Re}\{z_{2,1}(x+t)e^{it}\}$ is zero (cf. (22) above), so the first order effect on the bifurcation parameter $\sigma = a_2(0)$ is zero as we move away from the two-hump traveling wave in the direction of $v^{(0)}$. The directional derivative of T in this direction is also zero, so the Liapunov-Schmidt reduction leads to an equation $g(\sigma, T) = 0$ such that $\frac{\partial g}{\partial T} = 0$ and $\frac{\partial g}{\partial \sigma} = 0$. By contrast, the first Fourier coefficient of $v^{(0)}(\cdot, 0)$ is non-zero and we do obtain a pitchfork bifurcation at F (and G) when we plot $a_1(0)$ vs. T, as was seen in Figure 4.

It turns out that the path of $a_2(0)$ vs. T from F to B is identical to the one from F to C; which one-hump stationary solution we end up with depends on whether we perturb the traveling wave in the direction of $+v^{(0)}$ or $-v^{(0)}$. However, there is another direction we can move while keeping G_{tot} zero (with $k = 2$ in (59)), namely $v^{(1)}(x,t) = \mathrm{Im}\{z_{2,1}(x+t)e^{it}\}$. This direction breaks the even symmetry of the initial condition, but the *even* Fourier modes still satisfy $b_k(0) = 0$ and $\partial_t a_k(0) = 0$; hence, the penalty function φ does not exclude this direction when $k = 2$ in (59). Depending on whether we perturb in the $+v^{(1)}$ or $-v^{(1)}$ direction, we end up at either the one-hump stationary solution E, with maximum at $x = 3\pi/2$, or D, with maximum at $x = \pi/2$. This shows that our choice of penalty function φ in (59) does not rule out non-trivial solutions with asymmetric initial conditions: the solutions on the path from (F or G) to (D or E) are all asymmetric at $t = 0$; however, these solutions are related to the ones on the path from (F or G) to (B or C) by a phase shift in space. We have not found any periodic solutions that cannot be made symmetric at $t = 0$ by such a phase shift.

In Figure 7, we show the trajectories of the second Fourier mode in the complex plane.

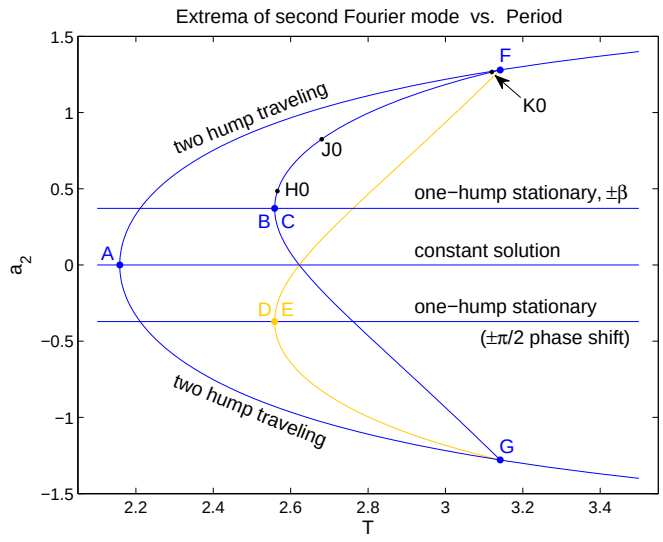

Figure 6: Bifurcation from the constant solution to a two-hump traveling wave and the path of non-trivial solutions connecting these to various one-hump stationary solutions.

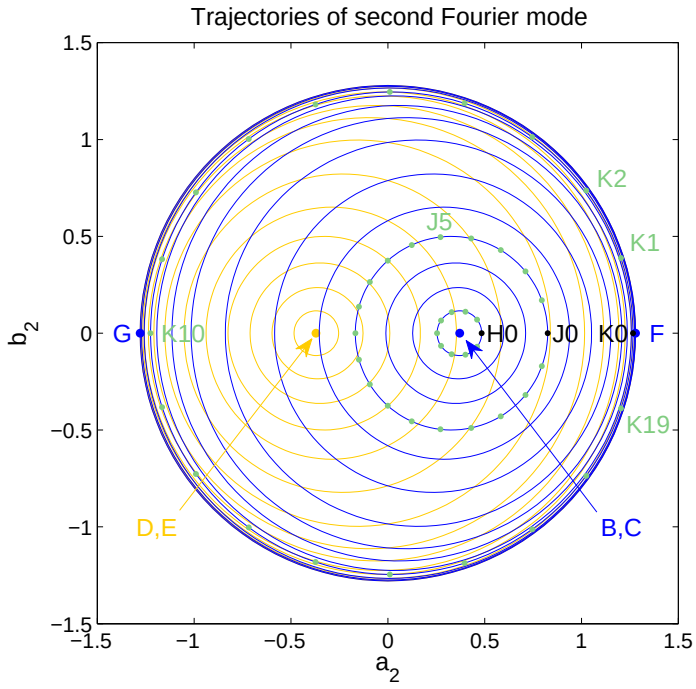

Figure 7: The trajectories of the second Fourier mode in the complex plane are epitrochoids; see Equation (62). The markers correspond to the solutions plotted in Figure 3.

The markers labeled H0, J0, etc. again correspond to the solutions plotted in Figure 3. Unlike the first Fourier mode, these trajectories are not exactly circular — but by curve fitting we determined they are epitrochoids, (resembling Ptolemy's model of planetary motion, or "spirograph" trajectories), of the form

$$c_2(t) = c_{20} + c_{2,-1}e^{i\omega t} + c_{2,-2}e^{i2\omega t}, \qquad (\omega = 2\pi/T)\,, \tag{62}$$

where the coefficients c_{2j} (and ω) depend on the bifurcation parameter σ. More generally, by curve fitting our numerical solutions, we have discovered a rather amazing property of solutions on this path: the kth Fourier mode is found to be of the form

$$c_k(t) = \sum_{j=-k}^{0} c_{kj}e^{-ij\omega t}, \qquad (k \geq 0,\ \omega = 2\pi/T), \tag{63}$$

where $c_{kj} \in \mathbb{R}$ and $c_{-k}(t) = \overline{c_k(t)}$. The general form of solutions on other paths connecting higher order bifurcations is similar, and is described in the follow-up paper [AW]. The four parameter family of non-trivial solutions is also nicely represented in this figure, where the parameters are the mean, the furthest point on the epitrochoid, a global rotation about the origin, and the choice of which point on the epitrochoid corresponds to $t = 0$. Note that a spatial phase shift of the initial condition by θ leads to a rotation of a trajectory in this figure clockwise by 2θ, so the north and south lobes of circles in Figure 5 collapse onto the west family of epitrochoids (around D and E) in Figure 7 while the west and east lobes of Figure 5 collapse onto the east family here.

6 Exact Solutions

The discovery that the Fourier modes execute Ptolemic orbits of the form (63) led us to expect that it might be possible to write down the solution in closed form. In this section, we show how to do this for the path of non-trivial solutions connecting the one-hump stationary solution to the two-hump traveling wave. Thus, we will prove existence of non-trivial time-periodic solutions by exhibiting a family of them explicitly. To our knowledge, this approach to constructing exact solutions of Benjamin-Ono is new, and is completely different from the methods described in [WLLZ05] or the references therein. In particular, Wang et. al. solve a projective Riccati equation to obtain exact solutions of a two-way, fourth order version of the Benjamin-Ono equation.

We start with the observation that if we are dealing with an N-soliton solution of the form

$$u(x,t) = \alpha_0 + \sum_{l=1}^{N} u_{\beta_l(t)}(x), \qquad \beta_l(t) \in \Delta \text{ satisfying (10)}, \tag{64}$$

then the first $N+1$ Fourier modes $c_k(t)$ of $u(x,t)$ are closely related to the trajectories of the β_l. Specifically, $\alpha_0 = c_0$ is needed to write down the ODE (10), and we have

$$\begin{aligned} \beta_1(t)+\cdots+\beta_N(t) &= s_1(t), & 2s_1(t) &= c_1(t), \\ \beta_1^2(t)+\cdots+\beta_N^2(t) &= s_2(t), & 2s_2(t) &= c_2(t), \\ &\cdots & & \\ \beta_1^N(t)+\cdots+\beta_N^N(t) &= s_N(t), & 2s_N(t) &= c_N(t). \end{aligned} \tag{65}$$

It is a standard theorem of algebra [vdW70] that the elementary symmetric functions

$$\sigma_j = \sum_{l_1<\cdots<l_j} \beta_{l_1}\cdots\beta_{l_j}, \qquad (j=1,\ldots,N) \tag{66}$$

are polynomials in the power sums, e.g.

$$\sigma_0 = 1, \qquad \sigma_1 = s_1, \qquad \sigma_2 = \frac{s_1^2 - s_2}{2}, \qquad \sigma_3 = \frac{s_1^3 - 3s_1s_2 + 2s_3}{6}. \tag{67}$$

The general recurrence relation is

$$\sigma_0 = 1, \qquad (-1)^j j\sigma_j + \sum_{k=0}^{j-1}(-1)^k \sigma_k s_{j-k} = 0, \qquad (j=1,\ldots,N). \tag{68}$$

The β_l are then the zeros of the polynomial

$$\prod_{l=1}^{N}(z-\beta_l(t)) = \sum_{j=0}^{N}(-1)^j\sigma_j(t)z^{N-j}. \tag{69}$$

Thus, we can test whether a given numerical solution $u(x,t)$ is an N-soliton solution by computing its first $N+1$ Fourier coefficients $c_k(0) = 2s_k(0)$, using (68) to obtain the symmetric functions $\sigma_j(0)$, solving for the roots $\beta_l(0)$ of the polynomial on the right hand side of (69), and checking that higher power sums do in fact agree with the Fourier coefficients of the solution:

$$\beta_1^k(0)+\cdots+\beta_N^k(0) = \frac{1}{2}c_k(0), \qquad (k \geq N+1). \tag{70}$$

Using this approach, we find (numerically) that the solutions on the path connecting the one-hump stationary solution to the two-hump traveling wave are 2-soliton solutions. Moreover, the trajectories of the first two symmetric functions appear to be of the form

$$\sigma_1 = \beta_1 + \beta_2 = -A + Be^{i\omega t}, \tag{71}$$

$$\sigma_2 = \beta_1\beta_2 \quad = -Ce^{i\omega t}, \tag{72}$$

where A, B, C, ω are positive constants; see Figure 8. We now prove this rigorously.

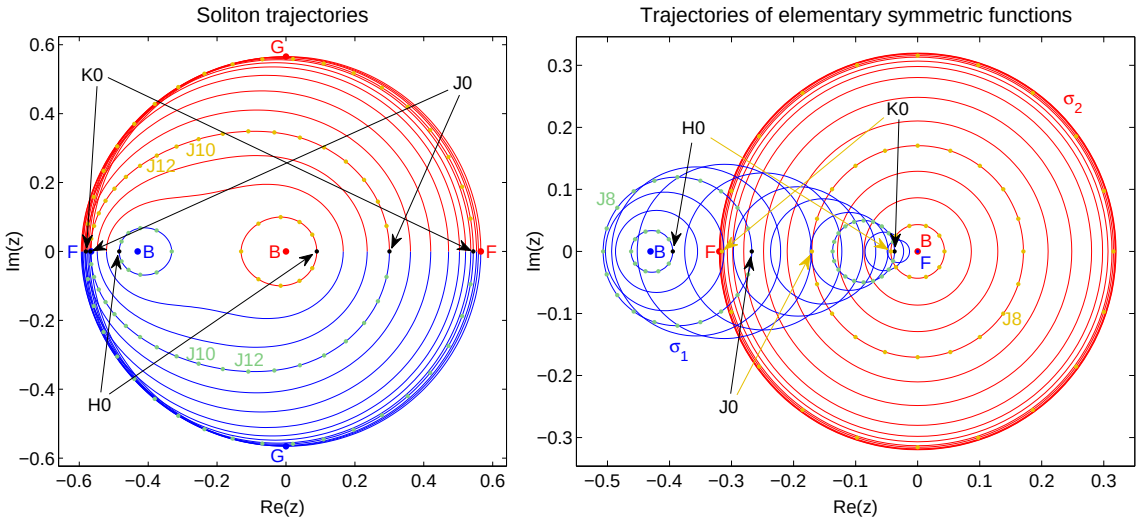

Figure 8: *Left:* trajectories of β_1, β_2 for the solutions in Figures 3–7. As we vary the bifurcation parameter, the trajectories change from two disjoint, counterclockwise loops to one larger orbit in which β_1, β_2 exchange positions over the course of one period. *Right:* the trajectories of σ_1, σ_2 are exactly circular.

THEOREM 1 *There is a four-parameter family of time-periodic, two-soliton solutions of the form*

$$u(x,t) = \alpha_0 + u_{\beta_1(t)}(x) + u_{\beta_2(t)}(x), \tag{73}$$

where $\beta_1(t)$ and $\beta_2(t)$ are the roots of the equation

$$z^2 - \sigma_1(t)z + \sigma_2(t) = 0 \tag{74}$$

and

$$\sigma_1(t) = [-A + Be^{i\omega(t-t_0)}]e^{-i\theta}, \qquad \sigma_2(t) = [-Ce^{i\omega(t-t_0)}]e^{-2i\theta}, \tag{75}$$

$$A = \frac{(3-\alpha_0)\sqrt{\left[(3-\alpha_0)-(7-\alpha_0)C^2\right]\left[(1-\alpha_0)-(5-\alpha_0)C^2\right]}}{(3-\alpha_0)^2-(5-\alpha_0)^2C^2}, \tag{76}$$

$$B = \frac{5-\alpha_0}{3-\alpha_0}AC, \tag{77}$$

$$\omega = \frac{(3-\alpha_0)^2-(5-\alpha_0)^2C^2}{(3-\alpha_0)-(5-\alpha_0)C^2}. \tag{78}$$

The four parameters are the mean $\alpha_0 < 1$, two phases $\theta, t_0 \in \mathbb{R}$, and a real number C ranging from $C = 0$ (at the one-hump stationary solution) to $C = \sqrt{\frac{1-\alpha_0}{5-\alpha_0}}$ (at the two-hump traveling wave).

PROOF: It suffices to prove this with $\theta = 0$ and $t_0 = 0$ as the general case follows immediately from this canonical case. If we try to substitute $\beta_{1,2} = \frac{\sigma_1}{2} \pm \frac{1}{2}\sqrt{\sigma_1^2 - 4\sigma_2}$ into the system

$$\dot\beta_1 = \frac{2i}{\beta_1^{-1} - \beta_2^{-1}} + \frac{2i\beta_1^2}{\beta_1 - \bar\beta_1^{-1}} + \frac{2i\beta_1^2}{\beta_1 - \bar\beta_2^{-1}} + i(1-\alpha_0)\beta_1 \tag{79}$$

$$\dot\beta_2 = \frac{2i}{\beta_2^{-1} - \beta_1^{-1}} + \frac{2i\beta_2^2}{\beta_2 - \bar\beta_1^{-1}} + \frac{2i\beta_2^2}{\beta_2 - \bar\beta_2^{-1}} + i(1-\alpha_0)\beta_2 \tag{80}$$

and solve for A, B and ω in terms of C and α_0, the algebra becomes unmanageable. However, we can re-write this system in terms of σ_1 and σ_2 to obtain

$$\dot\sigma_1 = -2i\left\{\frac{\beta_1(\beta_1\bar\beta_1)}{1-\beta_1\bar\beta_1} + \frac{\beta_1(\beta_1\bar\beta_2)}{1-\beta_1\bar\beta_2} + \frac{\beta_2(\beta_2\bar\beta_1)}{1-\beta_2\bar\beta_1} + \frac{\beta_2(\beta_2\bar\beta_2)}{1-\beta_2\bar\beta_2}\right\} + i(1-\alpha_0)\sigma_1,$$

$$\dot\sigma_2 = -2i\left\{\frac{\beta_1\bar\beta_1}{1-\beta_1\bar\beta_1} + \frac{\beta_1\bar\beta_2}{1-\beta_1\bar\beta_2} + \frac{\beta_2\bar\beta_1}{1-\beta_2\bar\beta_1} + \frac{\beta_2\bar\beta_2}{1-\beta_2\bar\beta_2}\right\}\sigma_2 + i(4-2\alpha_0)\sigma_2.$$

The expressions inside braces remain invariant if we interchange β_1 and β_2; hence, they may be written as rational functions of σ_1, σ_2, $\bar\sigma_1$, $\bar\sigma_2$. Explicitly, we have

$$\dot\sigma_1 = -2i\frac{P_1}{Q} + i(1-\alpha_0)\sigma_1, \qquad \dot\sigma_2 = -2i\frac{P_2}{Q}\sigma_2 + i(4-2\alpha_0)\sigma_2, \tag{81}$$

$$P_1 = \sigma_1^2\bar\sigma_1 - 2\bar\sigma_1\sigma_2 - 2\sigma_1^3\bar\sigma_2 + 6\sigma_1|\sigma_2|^2 - \sigma_1\bar\sigma_1^2\sigma_2 + 2\sigma_1^2\bar\sigma_1|\sigma_2|^2 - 2\bar\sigma_1\sigma_2^2\bar\sigma_2 - 2\sigma_1|\sigma_2|^4,$$

$$P_2 = |\sigma_1|^2\big(1+3|\sigma_2|^2\big) + 4|\sigma_2|^2\big(1-|\sigma_2|^2\big) - 2\big(\sigma_1^2\bar\sigma_2 + \bar\sigma_1^2\sigma_2\big),$$

$$Q = \big(1-|\sigma_2|^2\big)^2 - |\sigma_1|^2\big(1+|\sigma_2|^2\big) + \big(\sigma_1^2\bar\sigma_2 + \bar\sigma_1^2\sigma_2\big).$$

Since Q is a product of non-zero terms of the form $(1-\beta_i\bar\beta_j)$, it is never zero. If we assume $\sigma_1 = -A + Be^{i\omega t}$, $\sigma_2 = -Ce^{i\omega t}$, and $C \neq 0$, we find that (81) holds as long as

$$\Big[-2P_1 + (1-\alpha_0)\sigma_1 Q\Big] + \frac{B}{C}\Big[-2P_2\sigma_2 + (4-2\alpha_0)\sigma_2 Q\Big] = 0, \tag{82}$$

$$-2P_2 + (4-2\alpha_0-\omega)Q = 0. \tag{83}$$

We eliminated ω in (82) using $\dot\sigma_1 = i\omega Be^{i\omega t} = -\frac{B}{C}\dot\sigma_2$. Next, we collect terms containing like powers of $e^{i\omega t}$ and set them each to zero. This yields 7 polynomial equations in the variables A, B, C, α_0 and ω; however, several of them are redundant due to relationships such as $Q^{(-1)} = Q^{(1)}$ in the decomposition $Q = Q^{(-1)}e^{-i\omega t} + Q^{(0)} + Q^{(1)}e^{i\omega t}$. Equation (82) yields 4 such equations; two of them are satisfied if we choose B as in (77) while the remaining two are satisfied if we also choose A as in (76). With these choices, all three equations associated with (83) are satisfied provided ω satisfies (78). The special cases $\{C=0,\ A=\sqrt{\frac{1-\alpha_0}{3-\alpha_0}},\ B=0\}$ and $\{C=\sqrt{\frac{1-\alpha_0}{5-\alpha_0}},\ A=0,\ B=0\}$ are seen to correspond to

the one-hump stationary solution and two-hump traveling wave, respectively, as discussed in Section 2. □

We have verified that the curve connecting B to F in the bifurcation diagram of Figure 4 is recovered if we set $\alpha_0 = .544375$ and plot $2(-A+B)$ versus $T = 2\pi/\omega$ using the above formulas for A, B and ω with C ranging from 0 to $\sqrt{\frac{1-\alpha_0}{5-\alpha_0}}$.

7 Conclusion

We have presented a general method for finding continua of time-periodic solutions for nonlinear systems of partial differential equations. We have used our method to study global paths of non-trivial time-periodic solutions connecting stationary and traveling waves of the Benjamin-Ono equation. Using Liapunov-Schmidt theory as a guide and linearizing about stationary and traveling waves, we determined that the manifold of non-trivial solutions is four dimensional with the mean, two phase-shifts and one essential bifurcation parameter describing the set of solutions. In spite of the non-linearity and non-locality of the Benjamin-Ono equation, these non-trivial solutions can be interpreted as distorted superpositions of the stationary or traveling waves at each end of the path. Our numerical method is accurate enough that we are able to use data fitting techniques to recognize the analytical form of the solutions. In particular, the Fourier coefficients $c_k(t)$ of these solutions follow "spirograph" orbits of the form (63). This led us to reformulate the equations governing the evolution of solitons to reveal an exact formula for the solutions on the four-parameter path connecting the one-hump stationary solution to the two-hump traveling wave.

In a follow-up paper [AW], we will classify all bifurcations from traveling waves, give several examples, and propose a conjecture about how they are connected together by paths of non-trivial solutions. We will also discuss blow-up of solutions (with the period T approaching zero as the bifurcation parameter approaches a critical value), and reformulate the problem in terms of a doubly-infinite sequence c_{kj} of unknown constants similar in form to (63). This reformulation leads to an interesting non-linear eigenvalue problem involving a two dimensional lattice sum, or convolution. Solutions of the lattice sum problem are closely related to the trajectories of solitons, and can likely be used to find more complicated exact solutions than the two-soliton solutions presented here. We also find interior bifurcations from these already non-trivial solutions. Thus, starting with the bifurcation from constant solutions to traveling waves, there may be an infinite cascade of bifurcations leading to more and more complicated time periodic solutions that nevertheless have algebraic formulas for the time-evolution of their Fourier modes and soliton positions.

In the future, we plan to apply this method to more complicated systems arising in fluid

dynamics, namely the vortex sheet and water wave problems. This will allow for comparison with prior numerical and analytical results [HLS97], [PT01], [IPT05]. Additionally, as the Benjamin-Ono equation is meant as a model for water waves on deep water, it will be of interest to compare time-periodic water waves of infinite depth with time-periodic solutions of Benjamin-Ono.

References

[Are63] R. F. Arenstorf. Periodic solutions of the restricted three body problem representing analytic continuations of Keplerian elliptic motions. *Amer. J. Math.*, LXXXV:27–35, 1963.

[AW] D. M. Ambrose and J. Wilkening. Global paths of time-periodic solutions of the Benjamin-One equation connecting arbitrary traveling waves. (in preparation).

[Ben67] T.B. Benjamin. Internal waves of permanent form in fluids of great depth. *J. Fluid Mech.*, 29:559–592, 1967.

[BGP98] M. O. Bristeau, R. Glowinski, and J. Périaux. Controllability methods for the computation of time-periodic solutions; application to scattering. *J. Comput. Phys.*, 147:265–292, 1998.

[Bre83] H. Brezis. Periodic solutions of nonlinear vibrating strings and duality principles. *Bull. Amer. Math. Soc. (N.S.)*, 8:409–426, 1983.

[Bro70] C. G. Broyden. The convergence of a class of double-rank minimization algorithms, Parts I and II. *J. Inst Maths Applics*, 6:76–90, 222–231, 1970.

[Cas78] K. M. Case. The N-soliton solution of the Benjamin–Ono equation. *Proc. Natl. Acad. Sci. USA*, 75(8):3562–3563, 1978.

[Cas80] K. M. Case. The Benjamin–Ono equation: a remarkable dynamical system. *Annals of Nuclear Energy*, 7:273–277, 1980.

[CI05] M. Chen and G. Iooss. Standing waves for a two-way model system for water waves. *European J. Mech. B/Fluids*, 24:113–124, 2005.

[CR04] M. Cabral and R. Rosa. Chaos for a damped and forced KdV equation. *Physica D*, 192:265–278, 2004.

[Cra96] A. Crannell. The existence of many periodic non-travelling solutions to the Boussinesq equation. *J. Differential Equations*, 126:169–183, 1996.

[CS83] G. J. Cooper and A. Sayfy. Additive runge-kutta methods for stiff ordinary differential equations. *Math. Comp.*, 40(161):207–218, 1983.

[DA67] R.E. Davis and A. Acrivos. Solitary internal waves in deep fluid. *J. Fluid Mech.*, 29:593–607, 1967.

[Dui84] J. J. Duistermaat. Bifurcations of periodic solutions near equilibrium points of Hamiltonian systems. In *Bifurcation Theory and Applications*, volume 1057 of *Lecture Notes in Mathematics*, pages 57–105. Springer, Berlin, 1984.

[FB85] Richard J. Field and Maria Burger. *Oscillations and Traveling Waves in Chemical Systems*. John Wiley and Sons, New York, 1985.

[Gov00] Willy J. F. Govaerts. *Numerical Methods for Bifurcations of Dynamical Equilibria*. SIAM, Philadelphia, 2000.

[GR06] R. Glowinski and T. Rossi. A mixed formulation and exact controllability approach for the computation of the periodic solutions of the scalar wave equation. (I): Controllability problem formulation and related iterative solution. *C. R. Acad. Sci. Paris, Ser. I*, 343:493–498, 2006.

[GS85] Martin Golubitsky and David G. Schaeffer. *Singularities and Groups in Bifurcation Theory*, volume I and II. Springer-Verlag, New York, 1985.

[GV91] J. Ginibre and G. Velo. Smoothing properties and existence of solutions for the generalized Benjamin-Ono equations. *J. Differential Equation*, 93:150–212, 1991.

[HLS94] T. Hou, J. Lowengrub, and M. Shelley. Removing the stiffness from interfacial flows with surface tension. *J. Comput. Phys.*, 114(2):312–338, 1994.

[HLS97] T. Hou, J. Lowengrub, and M. Shelley. The long-time motion of vortex sheets with surface tension. *Phys. Fluids*, 9(7):1933–1954, 1997.

[HNW00] Ernst Hairer, Syvert P. Norsett, and Gerhard Wanner. *Solving Ordinary Differential Equations I: Nonstiff Problems*. Springer, Berlin, 2nd edition, 2000.

[IPT05] G. Iooss, P.I. Plotnikov, and J.F. Toland. Standing waves on an infinitely deep perfect fluid under gravity. *Arch. Rat. Mech. Anal.*, 177:367–478, 2005.

[KC03] C. A. Kennedy and M. H. Carpenter. Additive Runge-Kutta schemes for convection-diffusion-reaction equations. *Appl. Numer. Math.*, 44(1–2):139–181, 2003.

[Kie04] Hansjörg Kielhöfer. *Bifurcation Theory: An Introduction with Applications to PDEs*. Springer, New York, 2004.

[Maw95] J. Mawhin. Periodic solutions of some semilinear wave equations and systems: A survey. *Chaos, Solitons & Fractals*, pages 1651–1669, 1995.

[Nir01] Louis Nirenberg. *Topics in Nonlinear Functional Analysis*. American Mathematical Society, Providence, 2001.

[NW99] Jorge Nocedal and Stephen J. Wright. *Numerical Optimization*. Springer, New York, 1999.

[Ono75] H. Ono. Algebraic solitary waves in stratified fluids. *J. Phys. Soc. Japan*, 39:1082–1091, 1975.

[Pao01] C.V. Pao. Numerical methods for time-periodic solutions of nonlinear parabolic boundary value problems. *SIAM J. Numer. Anal.*, pages 647–667, 2001.

[Pir84] O. Pironeau. *Optimal Shape Design for Elliptic Systems*. springer-Verlag, New York, 1984.

[PT01] P.I. Plotnikov and J.F. Toland. Nash-Moser theory for standing water waves. *Arch. Rat. Mech. Anal.*, 159:1–83, 2001.

[Rab78] P. H. Rabinowitz. Periodic solutions of Hamiltonian systems. *Comm. Pure Appl. Math.*, 31:157–184, 1978.

[Rab82] P. H. Rabinowitz. Periodic solutions of Hamiltonian systems: A survey. *SIAM J. Math. Anal.*, 13:343–352, 1982.

[Sau79] J.C. Saut. Sur quelques generalisations de l'equation de Korteweg-deVries. *J. Math. Pures Appl.*, 58:21–61, 1979.

[Smi89] M.W. Smiley. Breathers and forced oscillations of nonlinear wave equations on $\mathbf{R}^3$. *J. Reine Angew. Math.*, 398:25–35, 1989.

[Smi90] M.W. Smiley. Numerical determination of breathers and forced oscillations of nonlinear wave equations. In *Computational solution of nonlinear system of equations*, volume 26 of *Lectures in Appl. Math.*, pages 605–617, Providence, RI, 1990. American Mathematical Society.

[Str00] Steven H. Strogatz. *Nonlinear Dynamics and Chaos*. Perseus Books Group, 2000.

[Tao04] T. Tao. Global well-posedness for the Benjamin-Ono equation in $H^1(\mathbf{R})$. *J. Hyperbolic Diff. Eq.*, 1:27–49, 2004.

[vdW70] B. L. van der Waerden. *Algebra*, volume 1. Unger, New York, 1970.

[Wil07a] J. Wilkening. An algorithm for computing Jordan chains and inverting analytic matrix functions. *Linear Algebra Appl.*, 427:6–25, 2007.

[Wil07b] Jon Wilkening. *Math 228A Lecture Notes: Numerical Solution of Differential Equations*. UC Berkeley, 2007. Available from author's webpage.

[WLLZ05] Zhen Wang, De-Sheng Li, Hui-Fang Lu, and Hong-Qing Zhang. A method for constructing exact solutions and application to Benjamin Ono equation. *Chinese Physics*, 14(11):2158–2163, 2005.

[Zeh83] E. Zehnder. Periodic solutions of Hamiltonian equations. In *Dynamics and Processes*, volume 1031 of *Lecture Notes in Mathematics*, pages 172–213. Springer, Berlin, 1983.